

# The Inside of Top Jets

---

---

**Gilad Perez**

**Weizmann Institute of Science**

*L. Almeida, S. Lee, G. Sterman, I. Sung, & J. Virzi, 0807.0234;*

*L. Almeida, S. Lee, I. Sung, & J. Virzi, 0810.0934;*

*Discussions with L. Almeida, S. Lee, J. Maldacena & G. Sterman.*

# Outline

---

---

- (very brief) Intro' top jets at the LHC.
- Jet mass:
  - (i) Signal & QCD BG (theory+MC);
  - (ii) Ex., SM:  $t\bar{t}$  vs. di-jet (via side band, th'+MC).
- Jet substructure, massive jet event shapes:
  - (i) Jet-Angularity;
  - (ii) Jet-Planarity;
  - (iii) Jet-Probe function (systematic approach).
- Summary.

# Introduction

---

- ◆ In the SM (& beyond) top is unique:
  - only ultra heavy quark,  $m_t \sim \langle H \rangle$ ;
  - induce most severe fine tuning;
  - controls flavor & custodial violation;
  - linked to EW breaking in natural models.
- ◆ Direct info' is limited (Tevatron).
- ◆ At the LHC:  $10^7$  tops/yr .
- ◆ SM: more than  $10^4$  tops/yr with  $\gamma_t \geq 5$ .

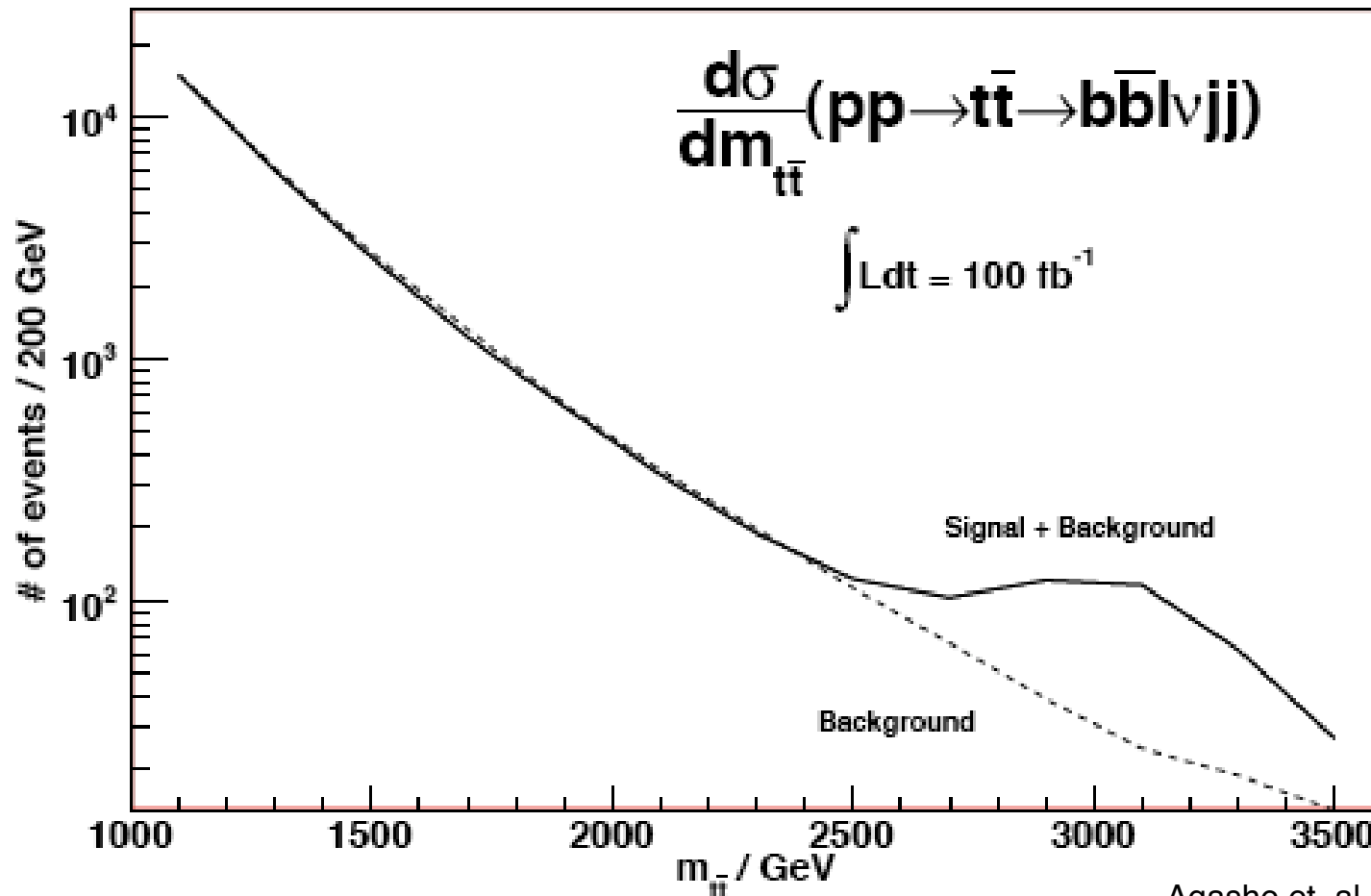
High  $p_t$  tops, might be crucial signal  
for various NP models

---

# High $p_t$ tops, might be crucial signal for various NP models

K. Agashe, A. Belyaev, T. Krupovnickas, G. Perez and J. Virzi, hep-ph/0612015;  
B. Lillie, L. Randall and L. T. Wang, hep-ph/0701166.

$$M_{KKG} = 3 \text{ TeV}$$

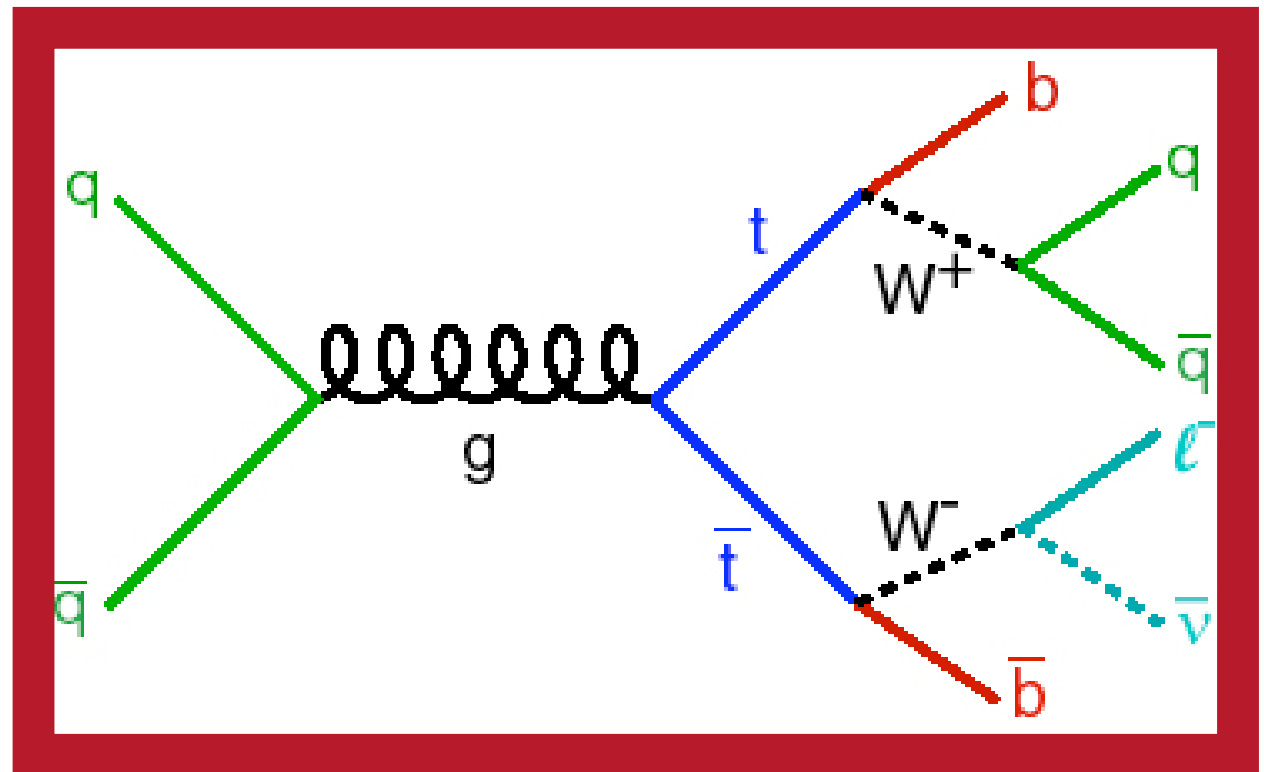


# The challenge of highly boosted tops

---

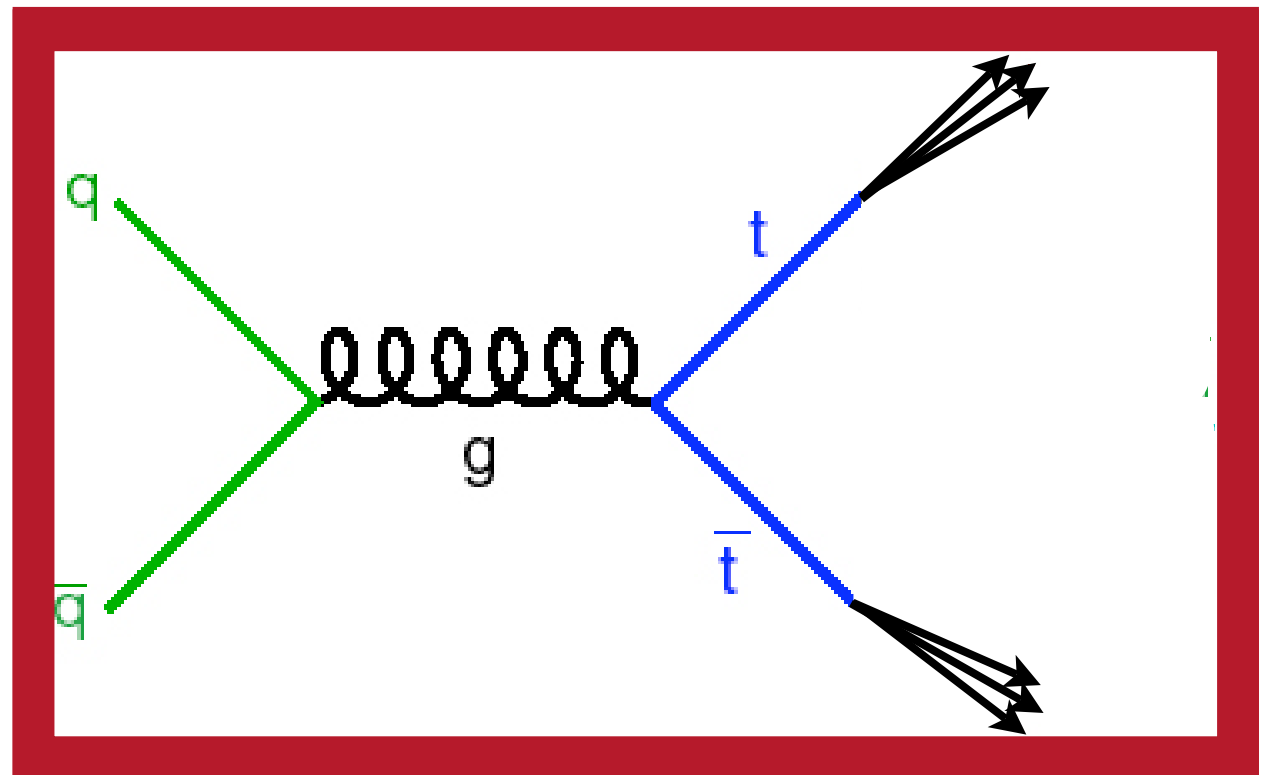
# The challenge of highly boosted tops

- Above a TeV, due to collimation, top's similar to light jet, efficiency & fake rate worsen.



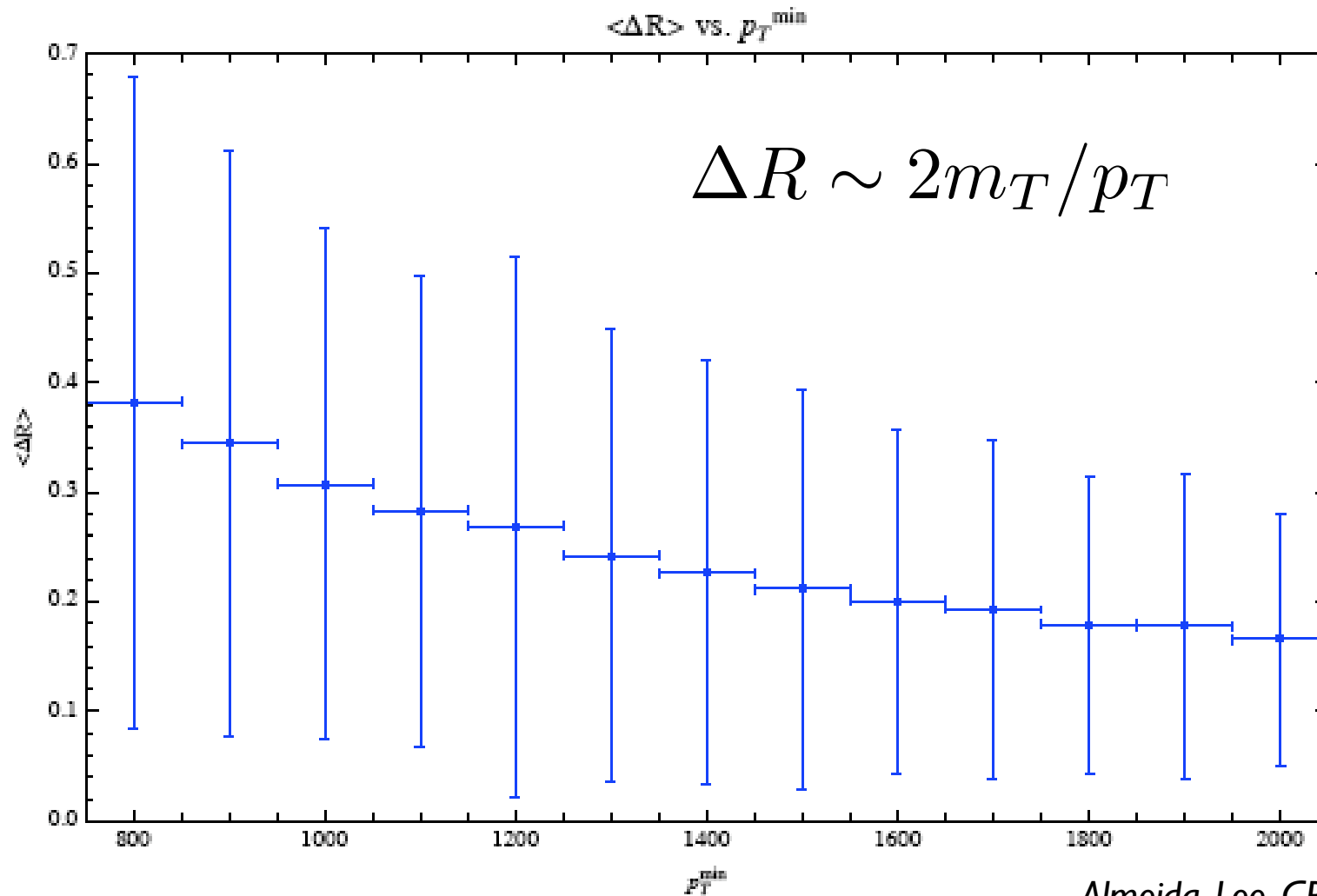
# The challenge of highly boosted tops

- Above a TeV, due to collimation, top's similar to light jet, efficiency & fake rate worsen.



- The concept of top jet emerges.

# Boosted top jets & collimation



Almeida, Lee, GP, Sung & Virzi (08).

Highly Boosted Tops:  
High Collimations!

$\Delta R$  vs.  $P_T$

# Why not use scaled-down conventional methods

---

- ◆ IRC (IR & collinear) safety require inclusive observables (e.g. cone or  $k_t$  jets).
- ◆ Hadronic calorimeter tower has an hard angular size  $R \sim 0.1$ .
- ◆ Radial shower of energetic hadrons are very large.

# Shower size of a single 100 GeV pion

◆ Ave' cone of 20 cm is required to contain 95% of the energy; a full cell size!

E% vs. size of section

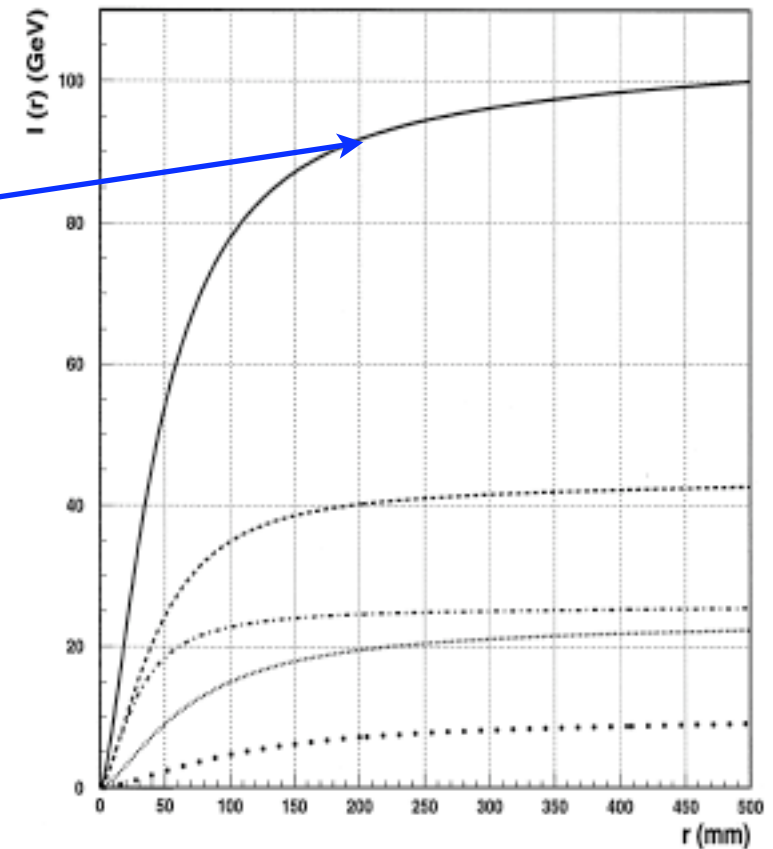


Fig. 14. Containment of shower  $I(r)$  (the solid line) as a function of radius for the entire Tile Calorimeter. The dash-dotted line is the contribution from the first depth segment, the dashed line is the contribution from the second depth segment, the thin dotted line is the contribution from the third depth segment, the thick dotted line is the contribution from the fourth depth segment.

# Shower size of a single 100 GeV pion

- ◆ Ave' cone of 20 cm is required to contain 95% of the energy; a full cell size!
- ◆  $R=0.4$  smallest cone used so far. A careful th'+exp' effort required to go beyond that.

E% vs. size of section

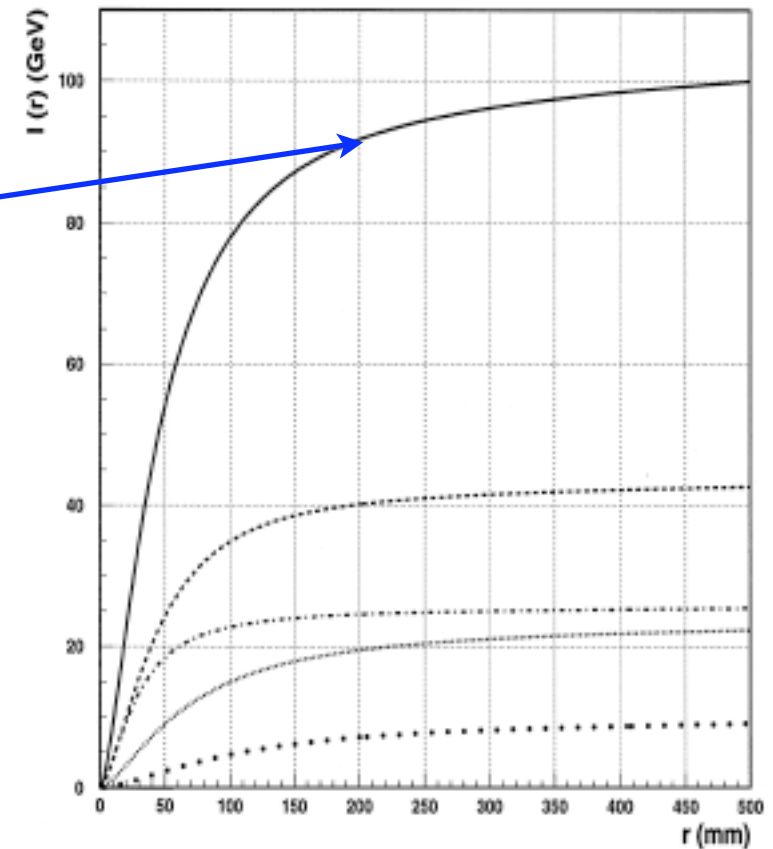


Fig. 14. Containment of shower  $I(r)$  (the solid line) as a function of radius for the entire Tile Calorimeter. The dash-dotted line is the contribution from the first depth segment, the dashed line is the contribution from the second depth segment, the thin dotted line is the contribution from the third depth segment, the thick dotted line is the contribution from the fourth depth segment.

# t-jets @ the LHC

“0th order”: t-jet = QCD jet

$S/B < 10^{-2}$ , for  $p_t(j) > 1000 \text{ GeV}$ ,  $R=0.4$

(10pb for  $jj+X$ , 100fb for  $t\bar{t}+X$ )

*Almeida, Lee, GP, Sung, & Virzi.*

Process	Generator	PDF	Matching	Cross Section
$pp \rightarrow t\bar{t}(j)$	SHERPA 1.0.9	CTEQ6M	CKKW	135 fb
$pp \rightarrow t\bar{t}(j)$	SHERPA 1.1.2	CTEQ6M	CKKW	149 fb
$pp \rightarrow t\bar{t}(j)$	MG/ME 4	CTEQ6M	MLM	68 fb
$pp \rightarrow t\bar{t}(j)$	MG/ME 4	CTEQ6L	MLM	56 fb
$pp \rightarrow t\bar{t}$	Pythia 6.4	CTEQ6L	-	157 fb
$pp \rightarrow t\bar{t}$	Pythia 8.1	CTEQ6M	-	174 fb
$pp \rightarrow jj(j)$	SHERPA 1.1.0	CTEQ6M	CKKW	10.2 pb
$pp \rightarrow jj(j)$	MG/ME 4	CTEQ6L	MLM	8.54 pb
$pp \rightarrow jj(j)$	MG/ME 4	CTEQ6M	MLM	9.93 pb
$pp \rightarrow jj$	Pythia 6.4	CTEQ6L	-	13.7 pb
$pp \rightarrow jj$	Pythia 8.1	CTEQ6M	-	13.3 pb

# t-jets @ the LHC

“0th order”: t-jet = QCD jet

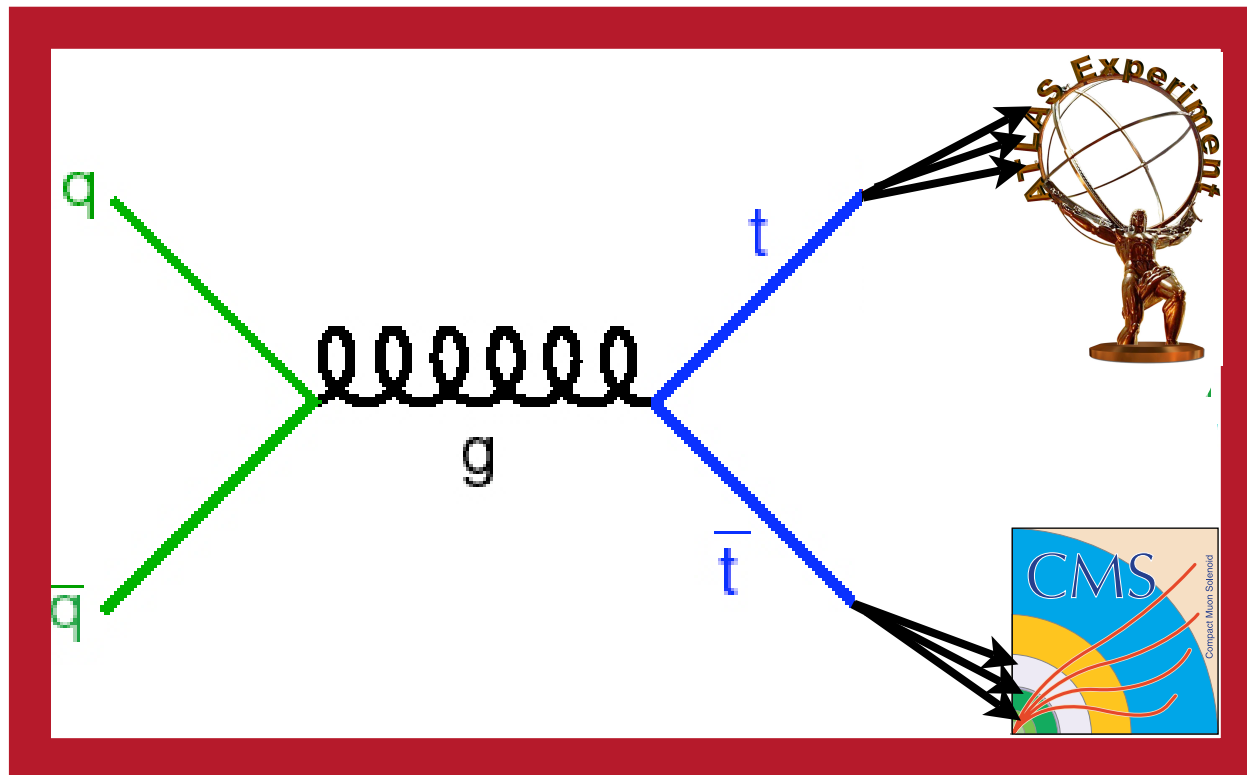
$S/B < 10^{-2}$ , for  $pt(j) > 1000 \text{ GeV}$ ,  $R=0.4$

(10pb for  $jj+X$ , 100fb for  $t\bar{t}+X$ )

*Almeida, Lee, GP, Sung, & Virzi.*

**t-jet**: call for theory,  
analysis & techniques.

# Top jets at the LHC



- (I) Jet mass.
- (II) Jet substructure:
  - (i) angularity (ii) planarity (iii) probe function.

# Jet Mass, Overview

---

- ◆ Jet cone mass-sum of “massless” momenta in h-cal inside the cone:  $m_J^2 = (\sum_{i \in R} P_i)^2$ ,  $P_i^2 = 0$
- ◆ Jet cone mass is non-trivial both for S & B.  
(naively: QCD jets are massless while top jets  $\sim m_t$ )

# Jet Mass, Overview

---

- ◆ Jet cone mass-sum of “massless” momenta in h-cal inside the cone:  $m_J^2 = \left(\sum_{i \in R} P_i\right)^2$ ,  $P_i^2 = 0$
- ◆ Jet cone mass is non-trivial both for S & B.
- ◆ Simple mass tagging fails. (counting in mass window)
- ◆ S&B distributions via 1st principles & compare to Monte-Carlo.
- ◆ Allow us to improve S/B.

# Non trivial cone t-jet mass distribution

---

- ◆ Naively the signal is  $J \propto \delta(m_J - m_t)$
- ◆ In practice:  $m_J^t \sim m_t + \delta m_{QCD} + \delta m_{EW}$

# Non trivial cone t-jet mass distribution

---

- ◆ Naively the signal is  $J \propto \delta(m_J - m_t)$
- ◆ In practice:  $m_J^t \sim m_t + \delta m_{QCD} + \delta m_{EW}$

Can understood  
perturbatively  
fast & small  $\sim 10\text{GeV}$

# Non trivial cone t-jet mass distribution

---

◆ Naively the signal is  $J \propto \delta(m_J - m_t)$

◆ In practice:  $m_J^t \sim m_t + \delta m_{QCD} + \delta m_{EW}$

Can understood  
perturbatively  
fast & small  $\sim 10\text{GeV}$

Pure kinematical  
bW(qq) dist'  
in/out cone  
longer  $\sim 0.2\text{GeV}$

# Non trivial cone t-jet mass distribution

---

◆ Naively the signal is  $J \propto \delta(m_J - m_t)$

◆ In practice:  $m_J^t \sim m_t + \delta m_{QCD} + \delta m_{EW}$

Can understood  
perturbatively  
fast & small  $\sim 10\text{GeV}$

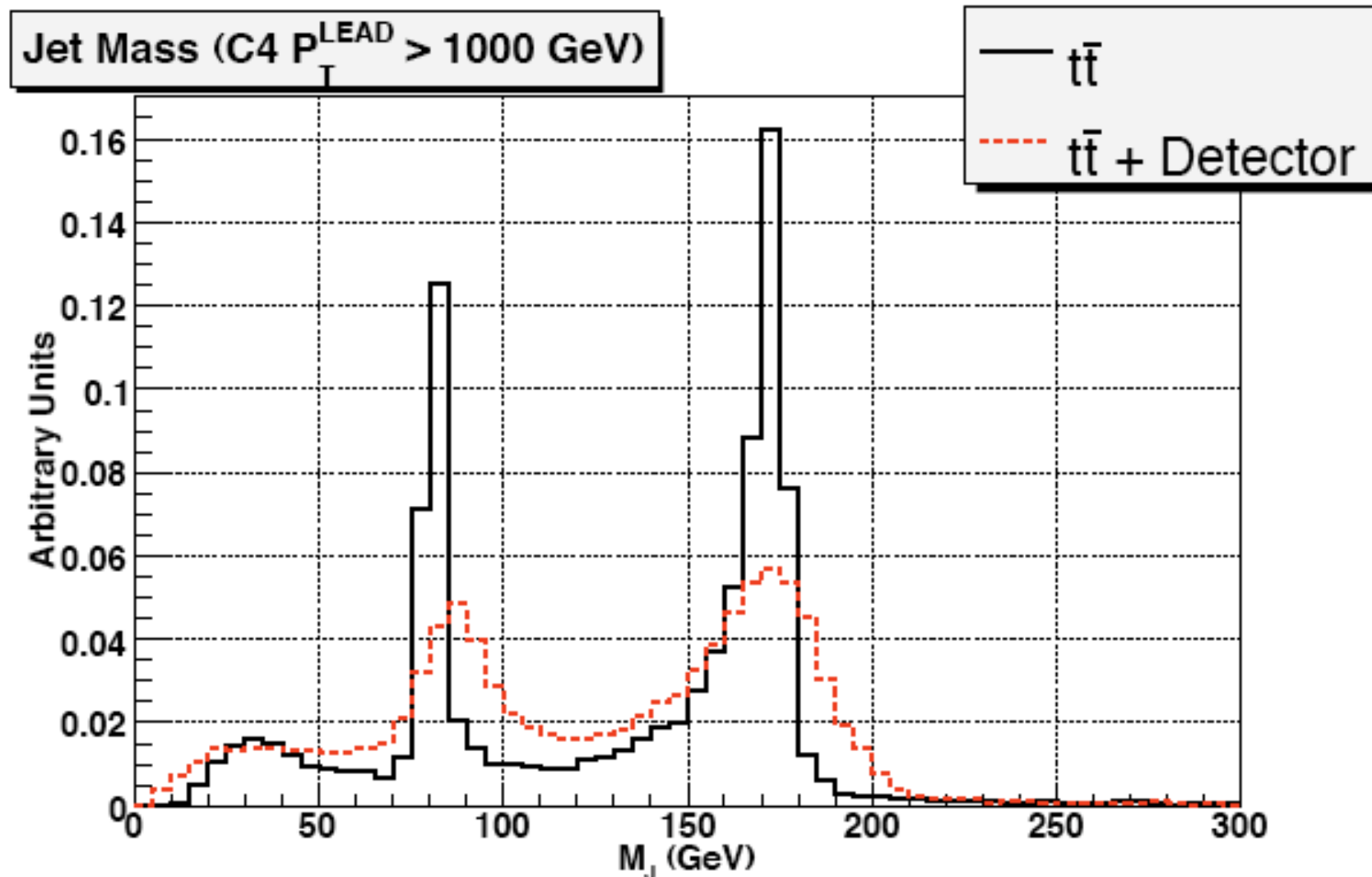
+ detector smearing.

Pure kinematical  
bW(qq) dist'  
in/out cone  
longer  $\sim 0.2\text{GeV}$

# Non trivial cone t-jet mass distribution

(Fleming, Hoang, Jain, Mantry, Scimemi, Stewart) Almeida, Lee, GP, Sung, & Virzi.

Sherpa => Transfer functions, JES  
(CKKW)



# QCD cone jet mass distribution

---

Boosted QCD Jet via factorization:

$$\frac{d\sigma^i}{dm_J} = J^i(m_J, p_T^{\min}, R^2) \sigma^i(p_T^{\min})$$
$$\int dm_J J^i = 1 \quad i = Q, G$$

Full expression:

$$\frac{d\sigma_{HAHB \rightarrow J_1 J_2}}{dm_{J_1}^2 dm_{J_2}^2 d\eta} = \sum_{abcd} \int dx_a dx_b \phi_a(x_a, p_T) \phi_b(x_b, p_T) \frac{d\hat{\sigma}_{ab \rightarrow cd}}{dp_T d\eta}(x_a, x_b, \eta, p_T)$$
$$S(m_{J_1}^2, m_{J_2}^2, \eta, p_T, R^2) J_1^{(c)}(m_{J_1}^2, \eta, p_T, R^2) J_2^{(d)}(m_{J_2}^2, \eta, p_T, R^2)$$

# QCD cone jet mass distribution

Boosted QCD Jet via factorization:

$$\frac{d\sigma^i}{dm_J} = J^i(m_J, p_T^{\min}, R^2) \sigma^i(p_T^{\min})$$

$i = Q, G$

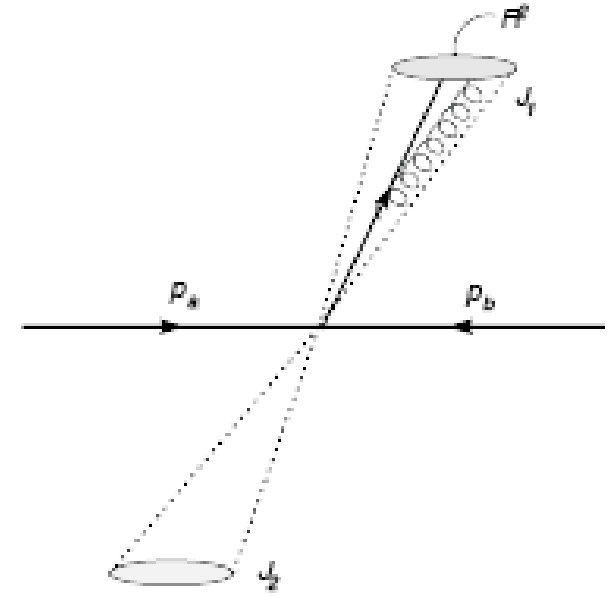
For large jet mass & small R,  
no big logs =>  
 $J^i$  can be calculated via  
perturbative QCD!

Full expression:

$$\frac{d\sigma_{HAHB \rightarrow J_1 J_2}}{dm_{J_1}^2 dm_{J_2}^2 d\eta} = \sum_{abcd} \int dx_a dx_b \phi_a(x_a, p_T) \phi_b(x_b, p_T) \frac{d\hat{\sigma}_{ab \rightarrow cd}}{dp_T d\eta}(x_a, x_b, \eta, p_T)$$
$$S(m_{J_1}^2, m_{J_2}^2, \eta, p_T, R^2) J_1^{(c)}(m_{J_1}^2, \eta, p_T, R^2) J_2^{(d)}(m_{J_2}^2, \eta, p_T, R^2)$$

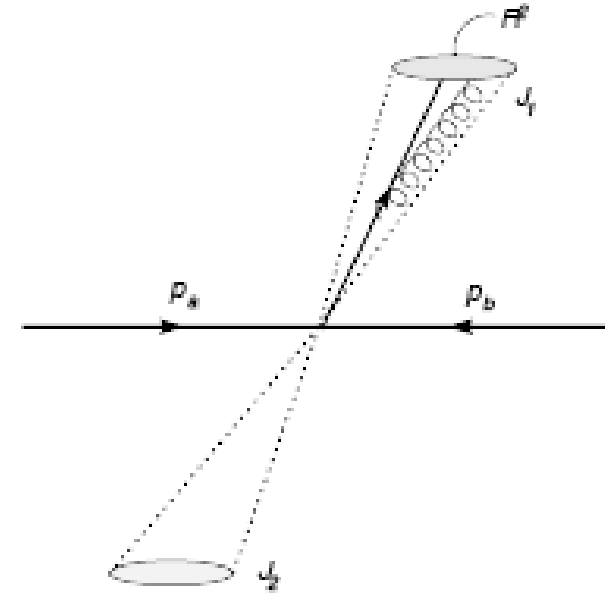
# QCD Jet mass distribution, Q+G

Main idea: calculating mass due to two-body QCD bremsstrahlung:



# QCD Jet mass distribution, Q+G

Main idea: calculating mass due to two-body QCD bremsstrahlung:



$$J^{(eik),c}(m_J, p_T, R) \simeq \alpha_S(p_T) \frac{4C_c}{\pi m_J} \log \left( \frac{R p_T}{m_J} \right)$$

$C_F = 4/3$  for quarks,  $C_A = 3$  for gluons.

# QCD Jet mass distribution, Q+G

---

$$J^{(eik),c}(m_J, p_T, R) \simeq \alpha_S(p_T) \frac{4C_c}{\pi m_J} \log\left(\frac{R p_T}{m_J}\right)$$

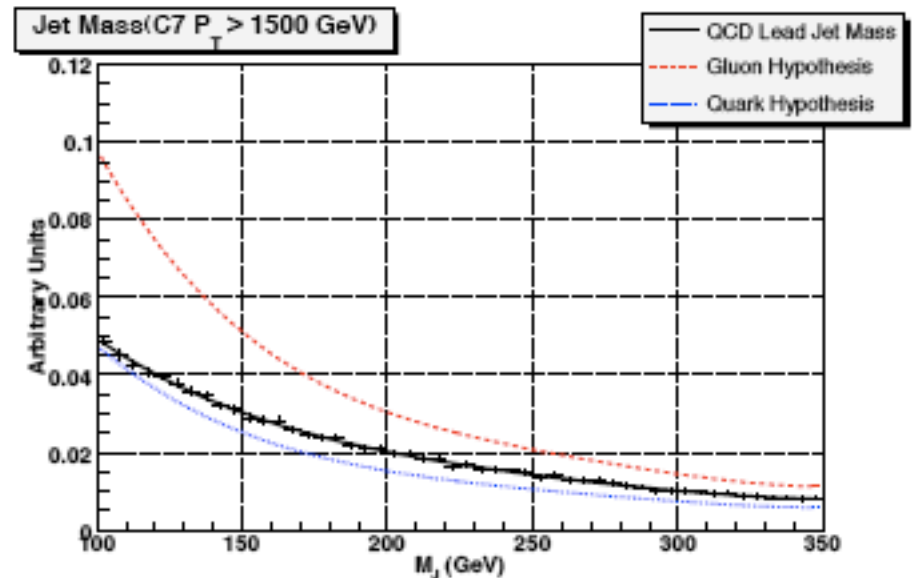
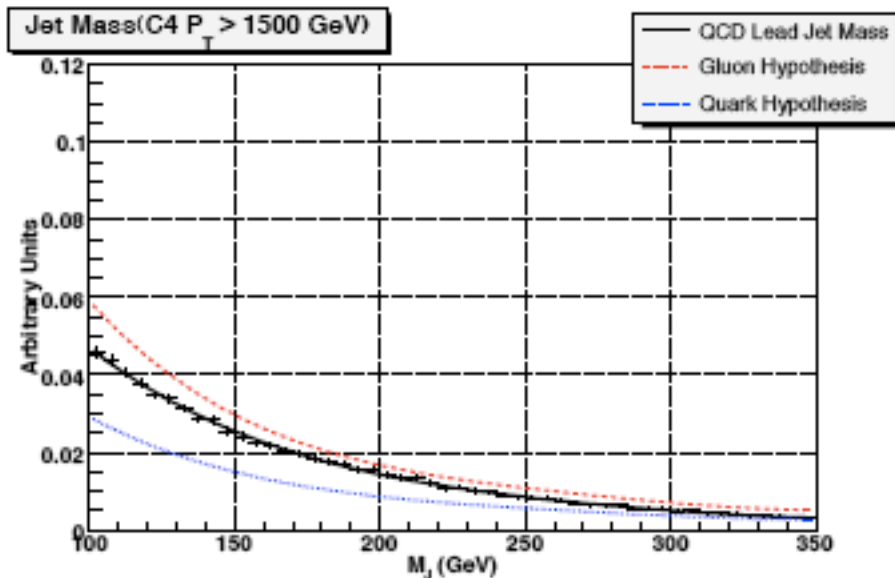
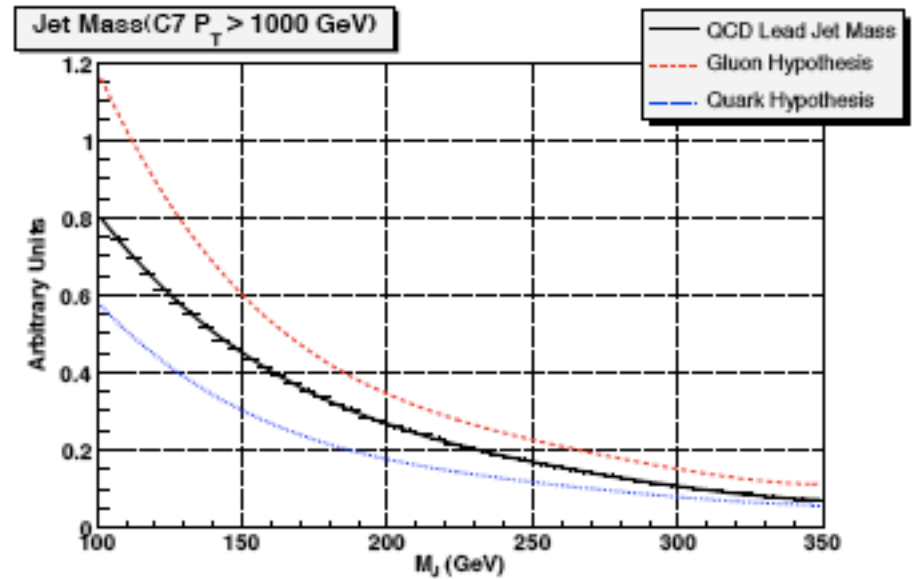
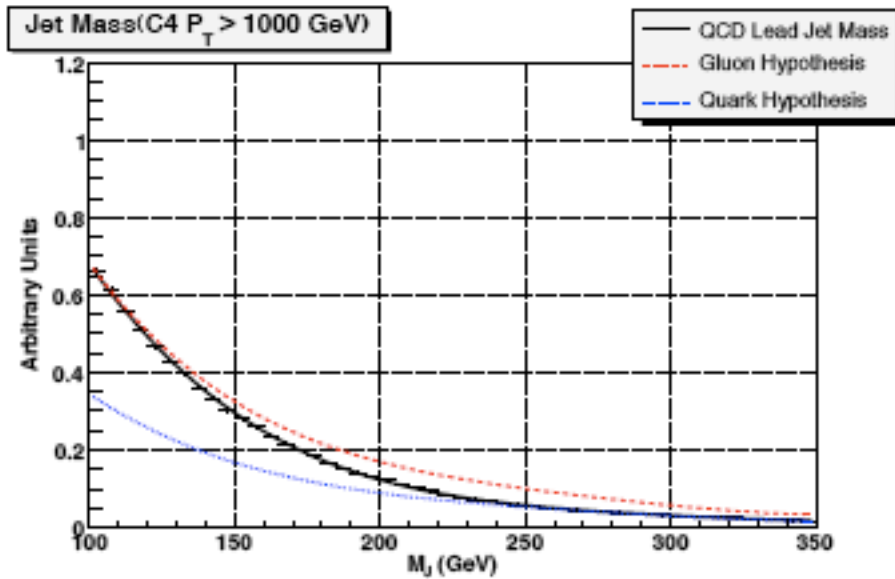
$C_F = 4/3$  for quarks,  $C_A = 3$  for gluons.

Data is admixture of the two, should be bounded by them:

$$\frac{d\sigma_{pred}(R)}{dp_T dm_J} \text{ upper bound} = J^g(m_J, p_T, R) \sum_c \left( \frac{d\sigma^c(R)}{dp_T} \right)_{MC},$$
$$\frac{d\sigma_{pred}(R)}{dp_T dm_J} \text{ lower bound} = J^q(m_J, p_T, R) \sum_c \left( \frac{d\sigma^c(R)}{dp_T} \right)_{MC},$$

# Jet mass distribution, theory vs. MC

Sherpa, jet function convolved above  $p_T^{\min}$



Ex.: SM  $t\bar{t}$  vs. di-jet



Ex.: SM  $t\bar{t}$  vs. di-jet



# SM $t\bar{t}$ vs. di-jet naive mass tagging

---

$p_T^{lead}$ cut	Cone Size	$t\bar{t}$ ( $S$ )	Background ( $B$ )	$S/B$
1000 GeV	C4	6860	113749	0.060
1000 GeV	C7	8725	197981	0.044
1500 GeV	C4	630	10985	0.057
1500 GeV	C7	689	13993	0.049

Sherpa Truth-level (no detector effects) results for single-tag jet mass method reflecting  $100 \text{ fb}^{-1}$  of integrated luminosity.

# SM $t\bar{t}$ vs. di-jet naive mass tagging

---

$p_T^{lead}$ cut	Cone Size	$t\bar{t}$ ( $S$ )	Background ( $B$ )	$S/B$
1000 GeV	C4	6860	113749	0.060
1000 GeV	C7	8725	197981	0.044
1500 GeV	C4	630	10985	0.057
1500 GeV	C7	689	13993	0.049

Sherpa Truth-level (no detector effects) results for single-tag jet mass method reflecting  $100 \text{ fb}^{-1}$  of integrated luminosity.

# SM $t\bar{t}$ vs. di-jet naive mass tagging

---

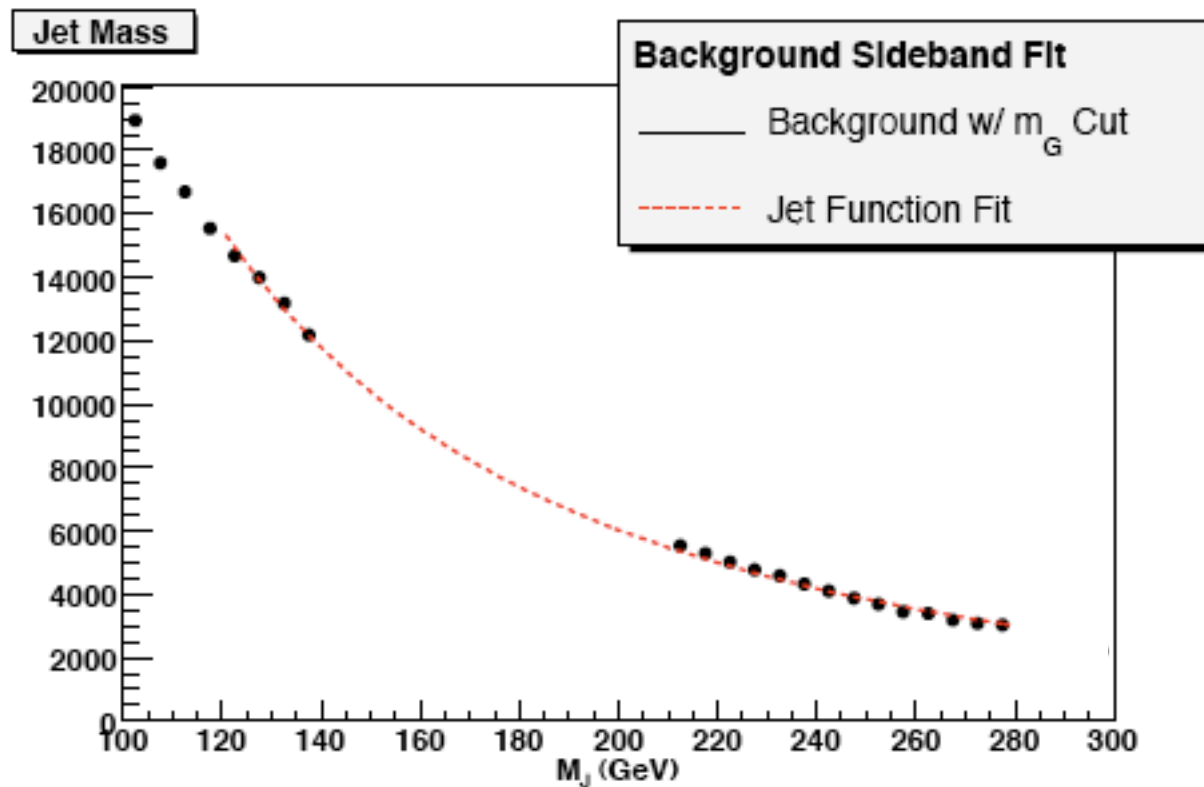
$p_T^{lead}$ cut	Cone Size	$t\bar{t}$ ( $S$ )	Background ( $B$ )	$S/B$
1000 GeV	C4	6860	113749	0.060
1000 GeV	C7	8725	197981	0.044
1500 GeV	C4	630	10985	0.057
1500 GeV	C7	689	13993	0.049

Sherpa Truth-level (no detector effects) results for single-tag jet mass method reflecting  $100 \text{ fb}^{-1}$  of integrated luminosity.

look hopeless  even with b-taggs!

# Remove background via side band analysis

Can use our understanding of background shapes to fit for the data.



A typical example of fitting jet functions to the jet mass distribution in the sideband regions  $(120 \text{ GeV} \leq m_J \leq 140 \text{ GeV}) \cup (210 \text{ GeV} < m_J < 280 \text{ GeV})$ . This plot corresponds to a single-tag analysis with C7 jets with  $p_T \geq 1000 \text{ GeV}$ .

# Remove background via side band analysis

---

Can use our understanding of background shapes to fit for the data. (only 4 input parameters, 18 bins)

$$F(m_J) = N_B \times b(m_J) + N_S \times s(m_J),$$

$$b(m_J) \propto \beta(m_J) \times J^Q(m_J; p_T^{\min}, R) + (1 - \beta(m_J)) \times J^G(m_J; p_T^{\min}, R),$$

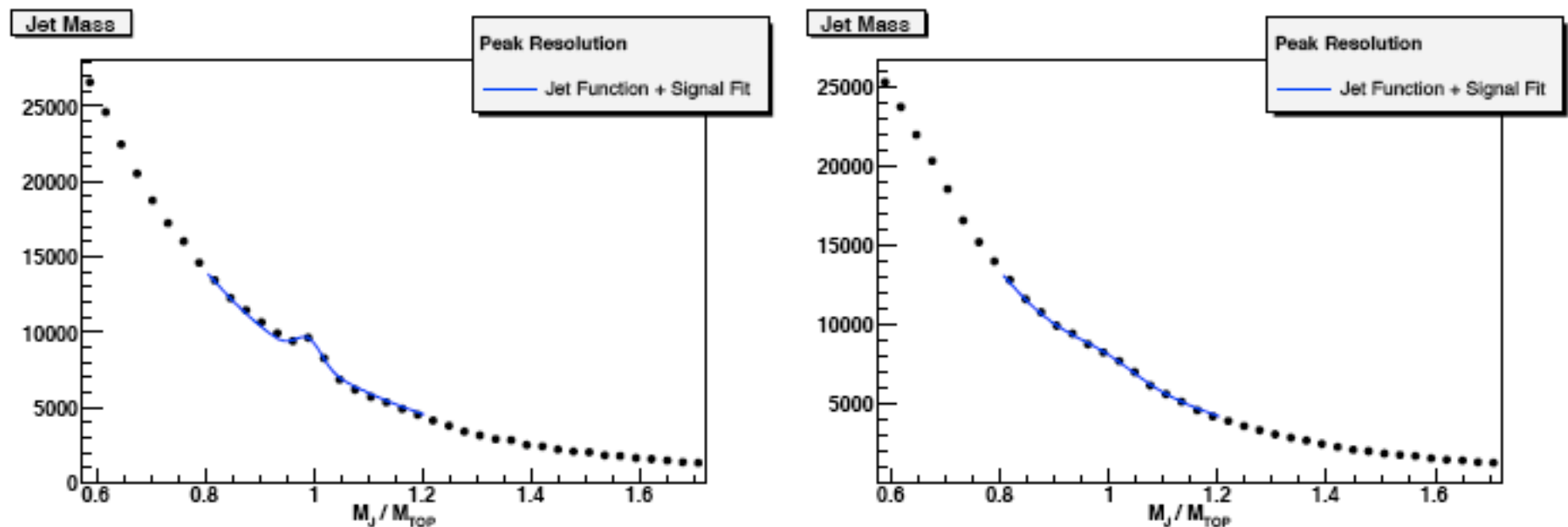
$$\text{where } \beta(m_J) \text{ is a linear polynomial } \left( \beta_0 + \beta_1 \frac{m_J}{p_T^{\min} R} \right).$$

Significance:  $n_\sigma = \sqrt{2 (\log \mathcal{L} - \log \mathcal{L}_0)},$

$$\mathcal{L} = \prod_{k=1}^{N_{\text{BINS}}} \frac{\exp(-F(m_k)) \times [F(m_k)]^{N_k}}{N_k!},$$

# Remove background via side band analysis

Can use our understanding of background shapes to fit for the data. (only 4 input parameters, 18 bins)



The results of fitting jet functions + signal shape to the jet mass distribution in the top mass window. The plot on the left corresponds to a truth-jet analysis. The plot on the right depicts the effects of detector smearing. The statistics reflect  $100 \text{ fb}^{-1}$  of integrated luminosity.

# Summary, mass tagging

---

Resolve signal from dijet background:

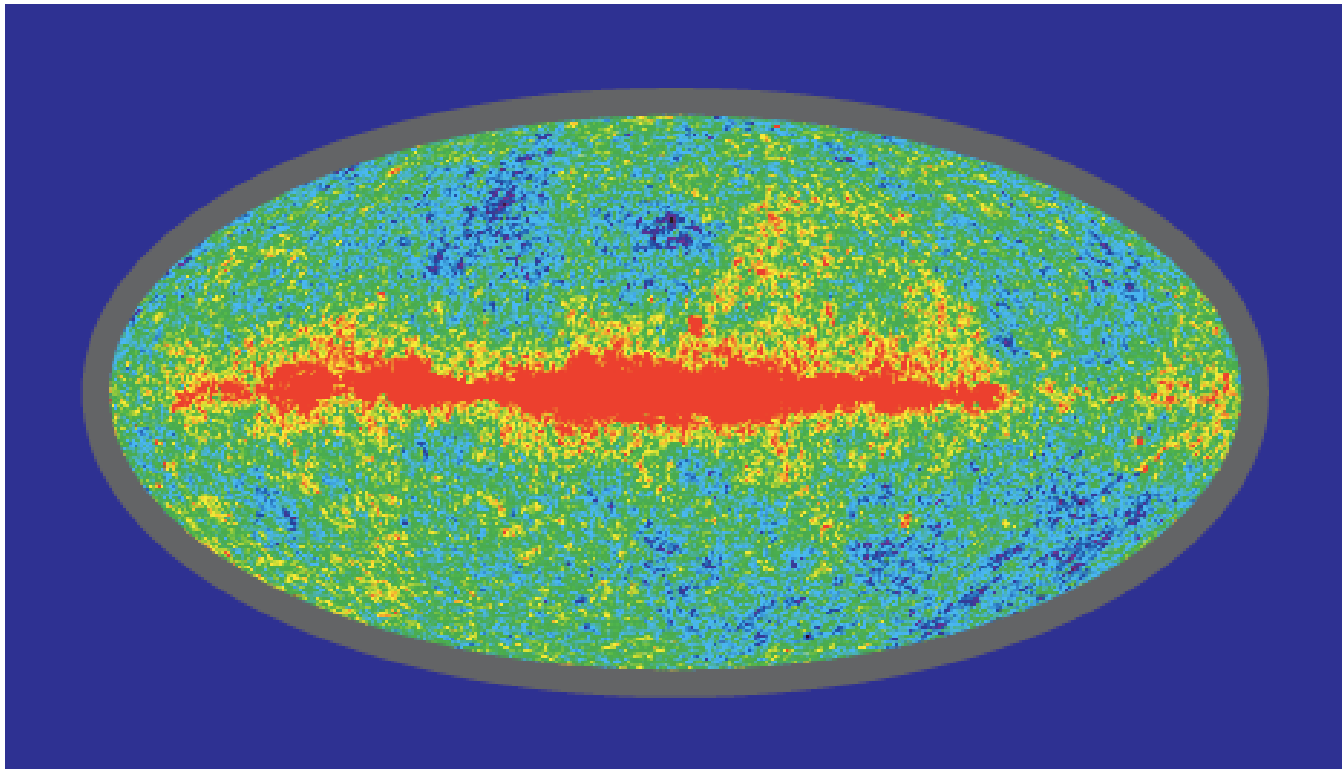
$$p_T^{min} \sim 1 \text{ TeV and } 25 \text{ fb}^{-1}$$

$$p_T^{min} \sim 1.5 \text{ TeV with } 100 \text{ fb}^{-1}$$

without jet substructure or b-tagging

Note that if  $S/B$  is enhanced,  
as in RS or other NP models reach is better.

# Jet sub-structure



*Almeida, Lee, GP, Sterman, Sung & Virzi; Brooijmans; Butterworth, et. al.;  
Thanler & Wang; Conway; Vos; Kaplan, Rehermann, Schwartz & Tweedie.*

# IRC-safe jet-shapes which know top from QCD jets?

---

◆ Successes in high jet mass  $\Rightarrow$  jet function is well described by single gluon radiation.

◆ As a warmup consider angularity (2-body final state):

Berger, Kucs and Sterman (03)

Angularities on a cone:

$$\tilde{\tau}_a(R, p_T) = \frac{1}{m_J} \sum_{i \in \text{jet}} \omega_i \sin^a \left( \frac{\pi \theta_i}{2R} \right) \left[ 1 - \cos \left( \frac{\pi \theta_i}{2R} \right) \right]^{1-a}$$

*Almeida, Lee, GP, Sterman, Sung, & Virzi.*

◆ Can evaluate distribution, fixing the mass  $\Rightarrow$  simplification.

# 2-body jet's kinematics, $Z/W/h$

---

$$P^x(\theta_s) = (dJ^x/d\theta_s)/J^x \Rightarrow P^x(\tilde{\tau}_a); \quad R(\tilde{\tau}_a) = \frac{P^{\text{sig}}(\tilde{\tau}_a)}{P^{\text{QCD}}(\tilde{\tau}_a)}$$

# 2-body jet's kinematics, $Z/W/h$

$$P^x(\theta_s) = (dJ^x/d\theta_s)/J^x \Rightarrow P^x(\tilde{\tau}_a); \quad R(\tilde{\tau}_a) = \frac{P^{\text{sig}}(\tilde{\tau}_a)}{P^{\text{QCD}}(\tilde{\tau}_a)}$$

$R^{\tau_{-2}}$  vs.  $\tau_{-2}$  for  $z=0.05$

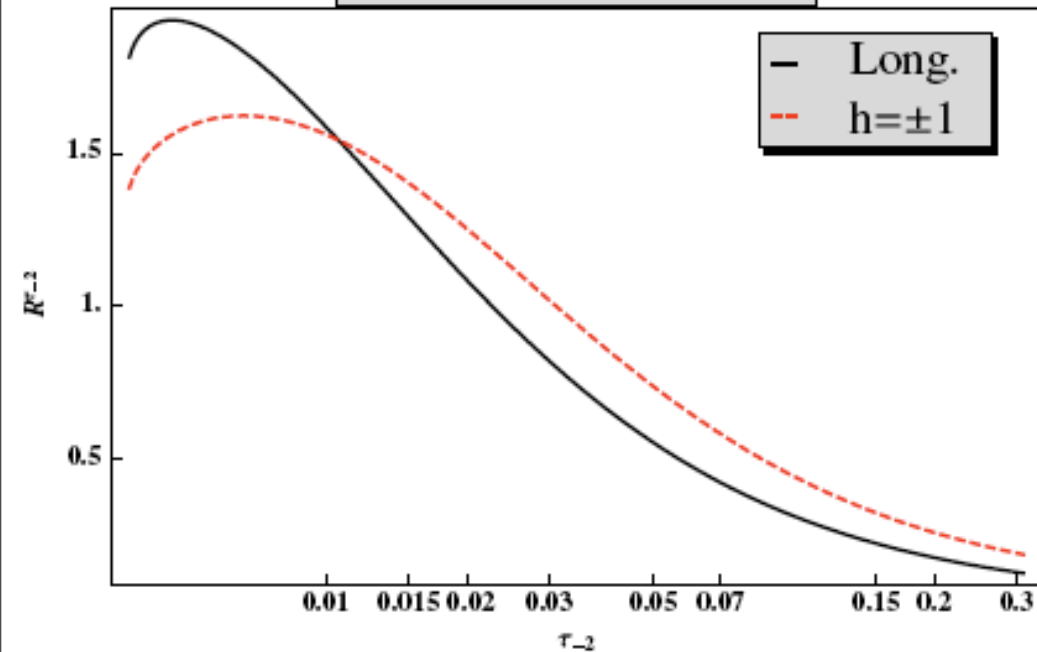


FIG. 3 (color online). The ratio between the signal and background probabilities to have jet angularity  $\tilde{\tau}_{-2}$ ,  $R^{\tilde{\tau}_{-2}}$ .

$$(z = m_J/p_T)$$

Angularity,  $\tau_a$  ( $a = -2$ ,  $z = 0.05$ ,  $R = 0.4$ )

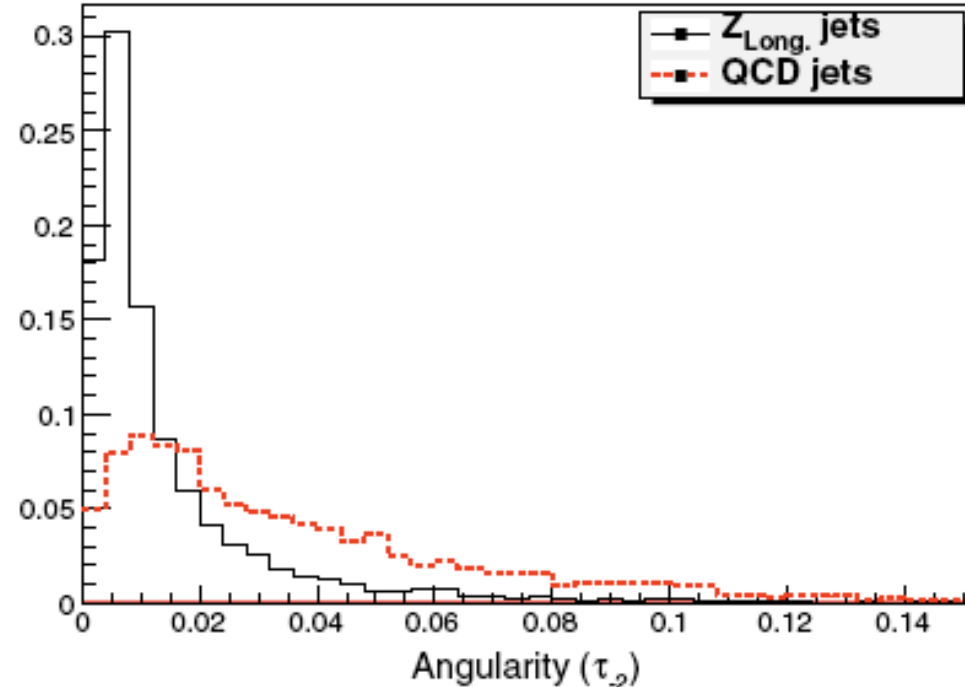


FIG. 4 (color online). The angularity distribution for QCD (red-dashed curve) and longitudinal Z (black-solid curve) jets obtained from MADGRAPH. Both distributions are normalized to the same area.

# 2-body jet's kinematics, $Z/W/h$

$$P^x(\theta_s) = (dJ^x/d\theta_s)/J^x \Rightarrow P^x(\tilde{\tau}_a); \quad R(\tilde{\tau}_a) = \frac{P^{\text{sig}}(\tilde{\tau}_a)}{P^{\text{QCD}}(\tilde{\tau}_a)}$$

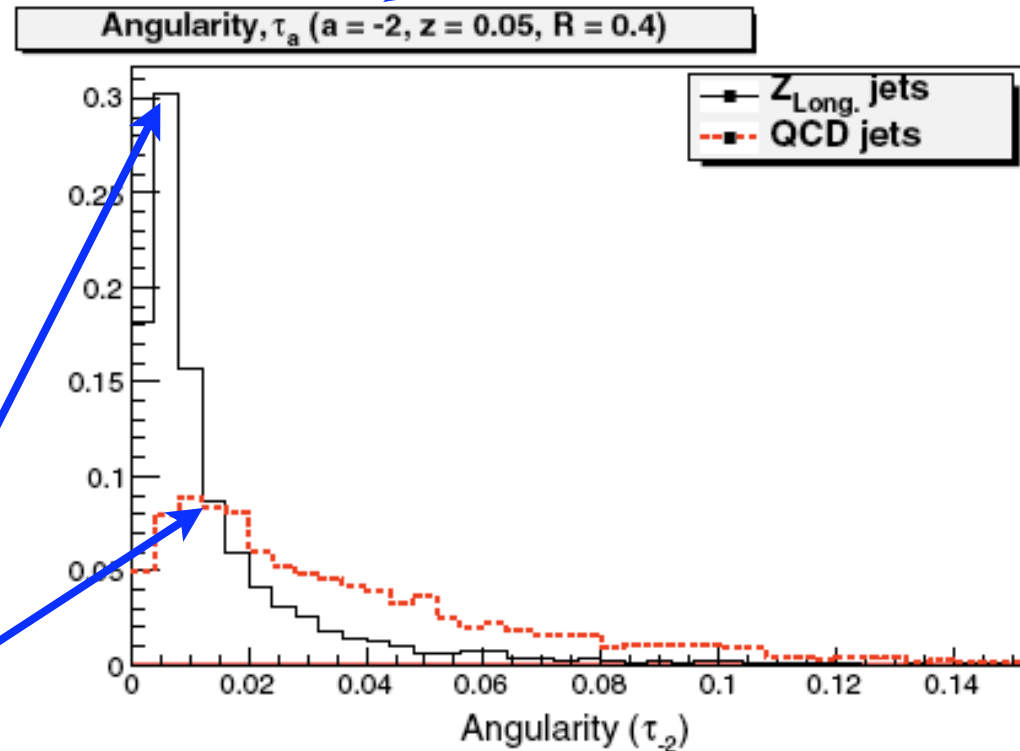
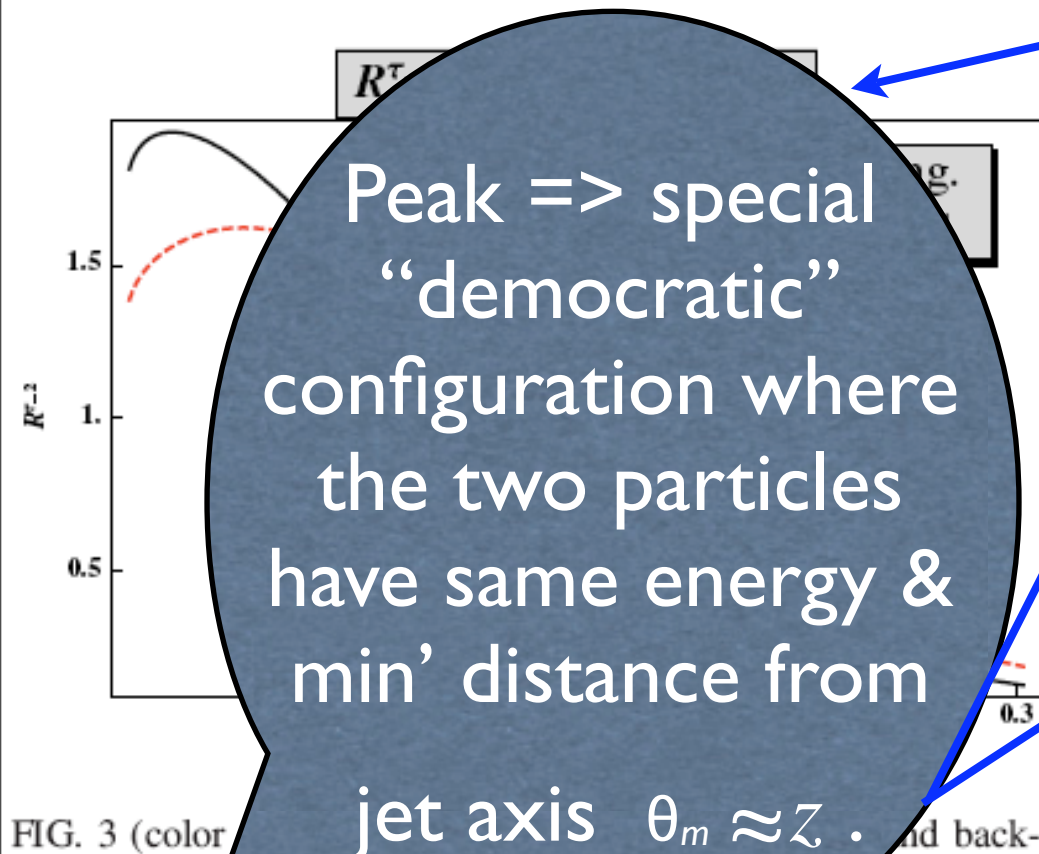


FIG. 4 (color online). The angularity distribution for QCD (red-dashed curve) and longitudinal Z (black-solid curve) jets obtained from MADGRAPH. Both distributions are normalized to the same area.

$$(z = m_J/p_T)$$

FIG. 3 (color online). Ground probability distribution and background probability distribution for 2-body jets.

# 2-body jet's kinematics, $Z/W/h$

t-jets are essentially different due to the  $W$  decay (3 body)

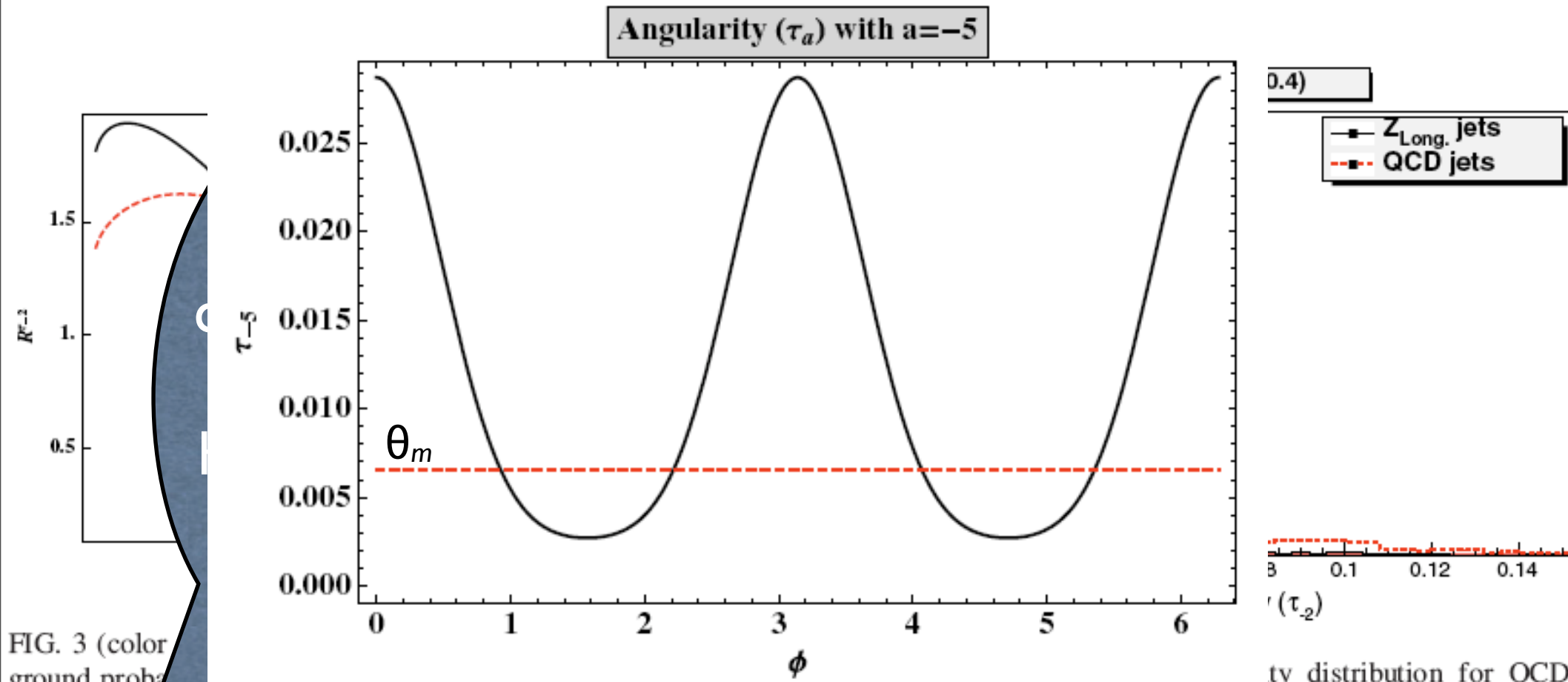


FIG. 3 (color ground proba

FIG. 5 (color online). Angularity,  $\tilde{\tau}_{-5}$  as a function of the azimuthal angle of the  $W(q\bar{q})$  pair,  $\phi_q$ , for a typical top jet event, compared to the typical case two-body kinematics.

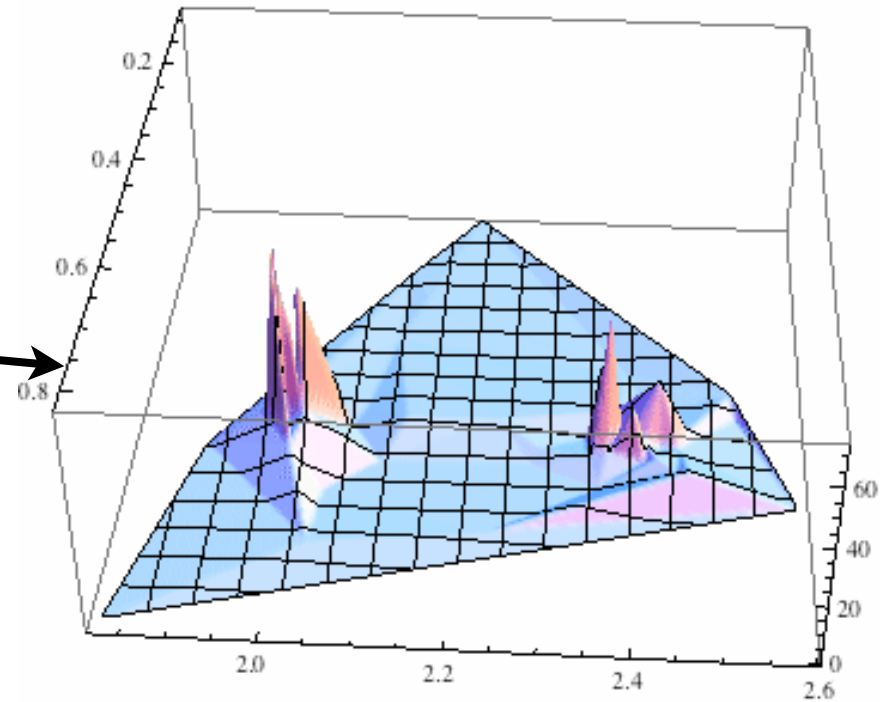
( $z =$

ty distribution for QCD  
 $Z$  (black-solid curve) jets  
 butions are normalized to

# QCD jets vs top jets via planar flow

◆ QCD jets are democratic & broad, shown both for cone & anti- $k_t$  jets.

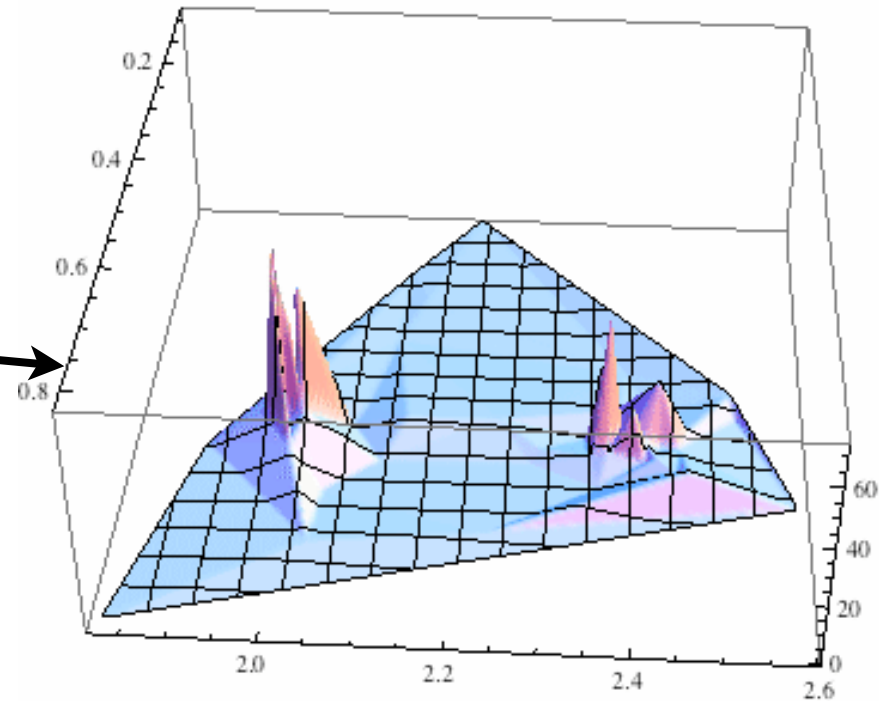
SISCone  
QCD Jet



# QCD jets vs top jets via planar flow

◆ QCD jets are democratic & broad, shown both for cone & anti- $k_t$  jets.

SISCone  
QCD Jet



◆ QCD, top: linear, planar E-deposition in the cone.

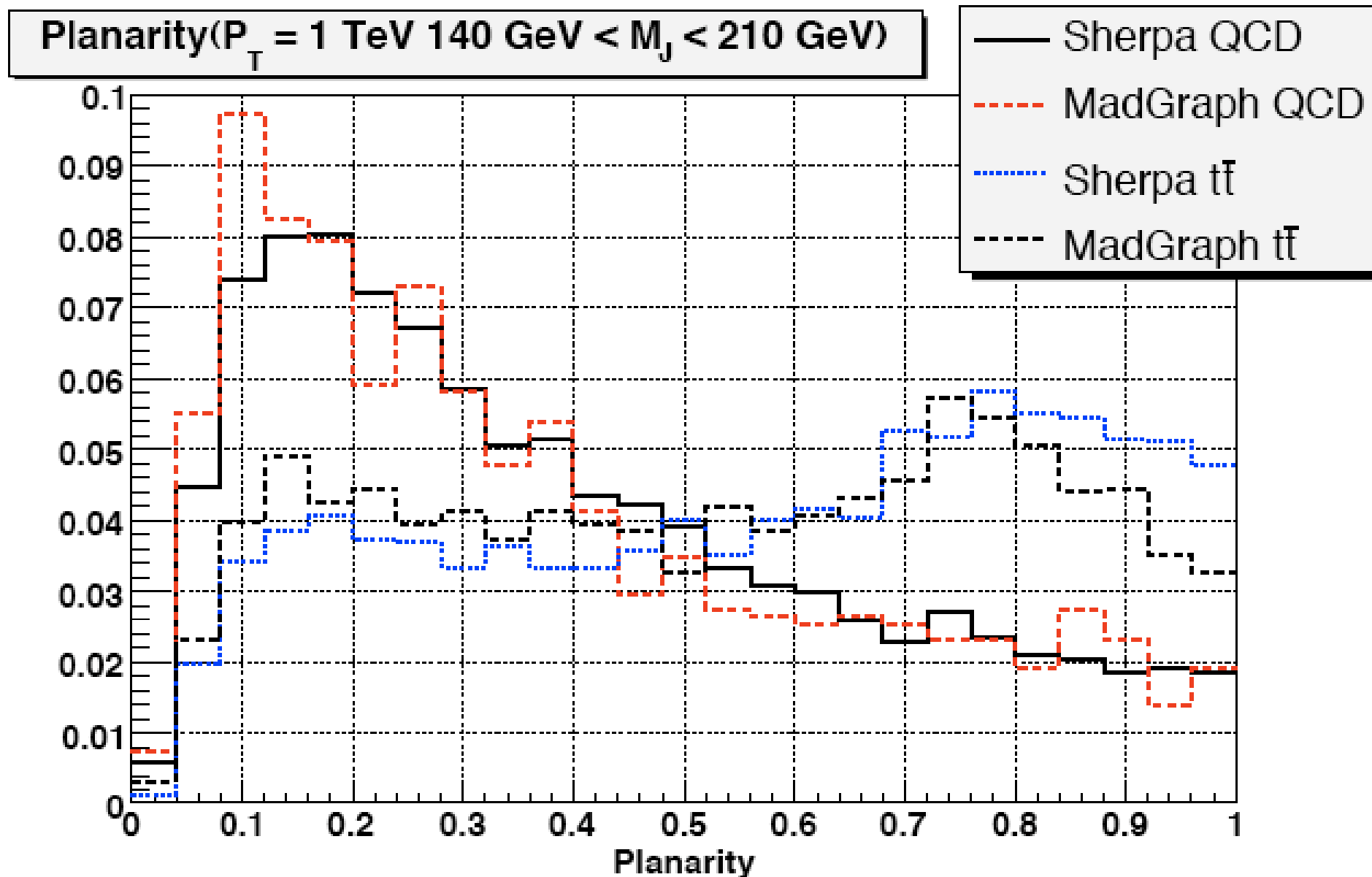
◆ IR-safe E-flow tensor: 
$$I_w^{kl} = \frac{1}{m_J} \sum_i w_i \frac{p_{i,k}}{w_i} \frac{p_{i,l}}{w_i}$$

◆ Planar flow: 
$$Pf = \frac{4 \det(I_w)}{\text{tr}(I_w)^2} = \frac{4\lambda_1 \lambda_2}{(\lambda_1 + \lambda_2)^2}$$

# Planar flow, QCD vs top jets

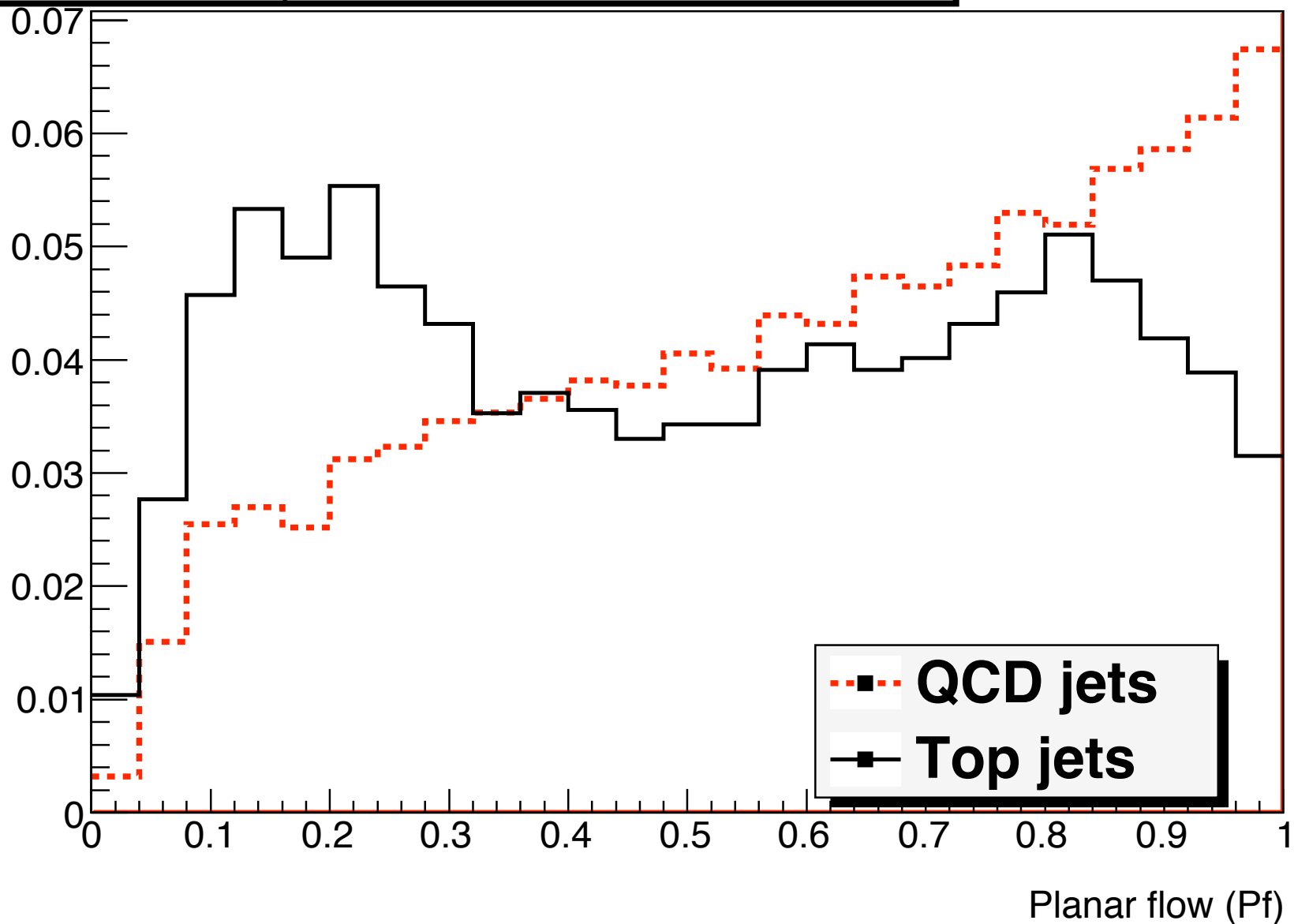
---

# Planar flow, QCD vs top jets

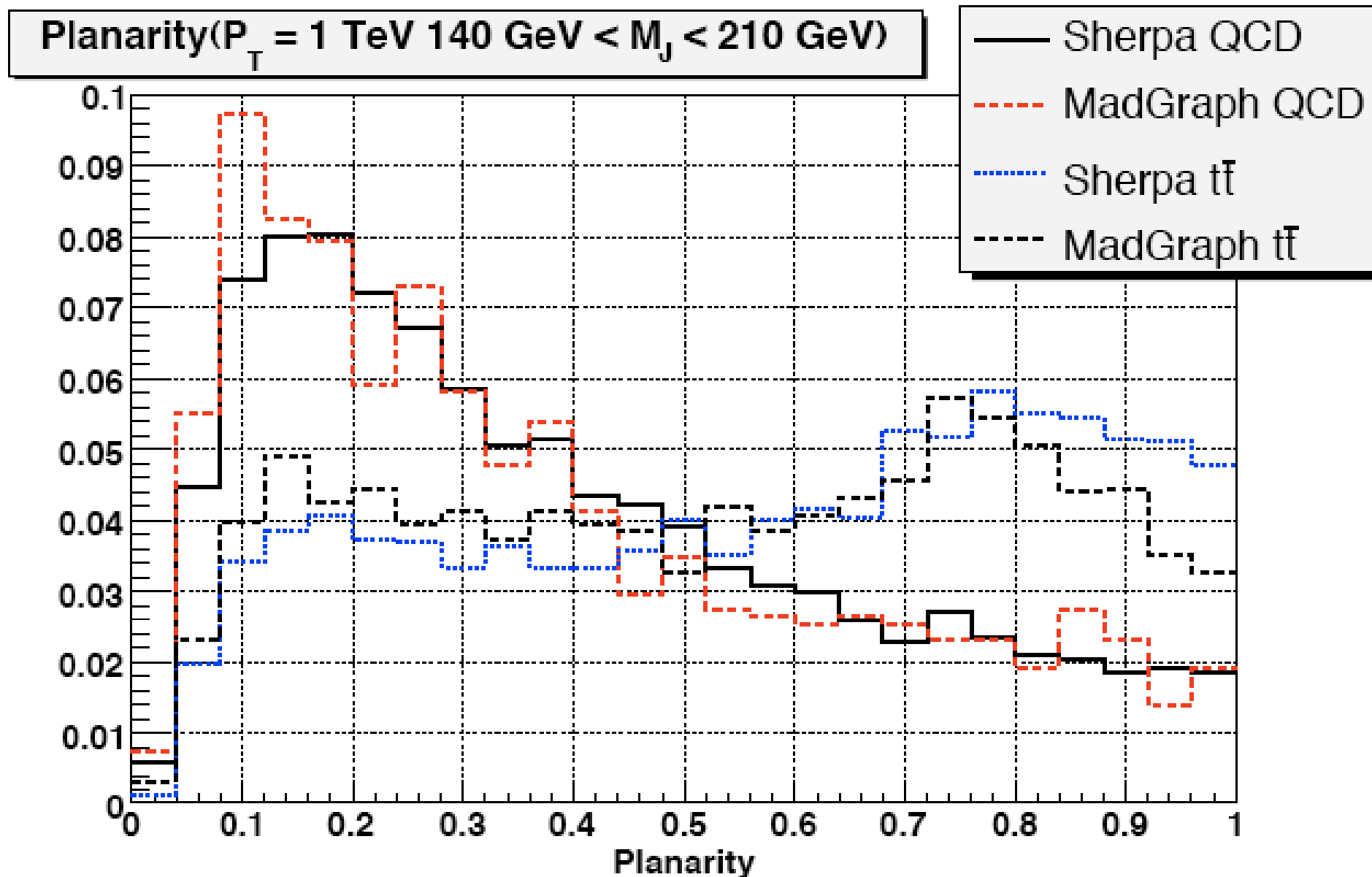


# Planar flow, QCD vs top jets

Planar flow, Pf ( $P_T = 1$  TeV,  $R = 0.4$ , "no mass cuts")

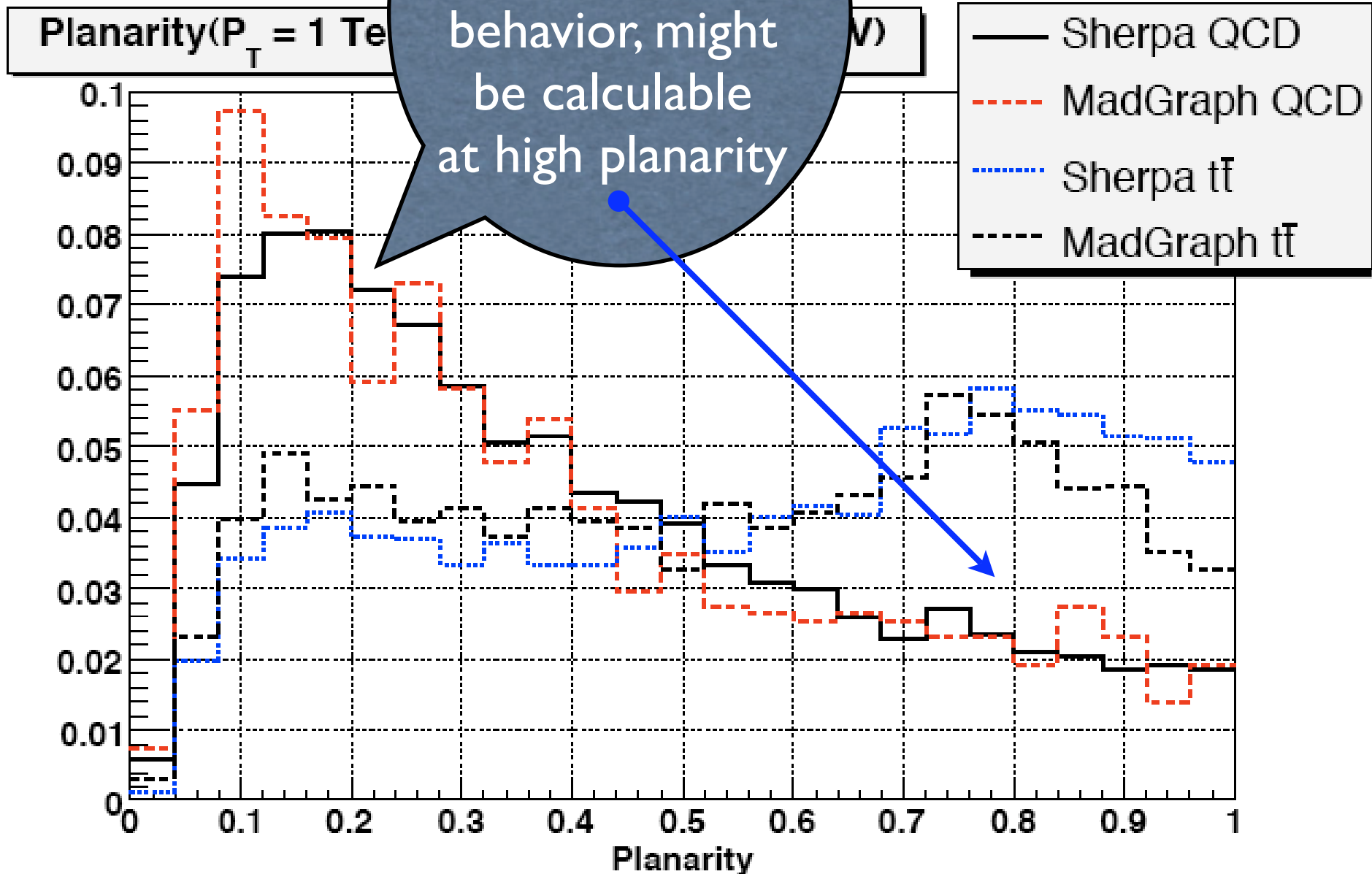


# Planar flow, QCD vs top jets

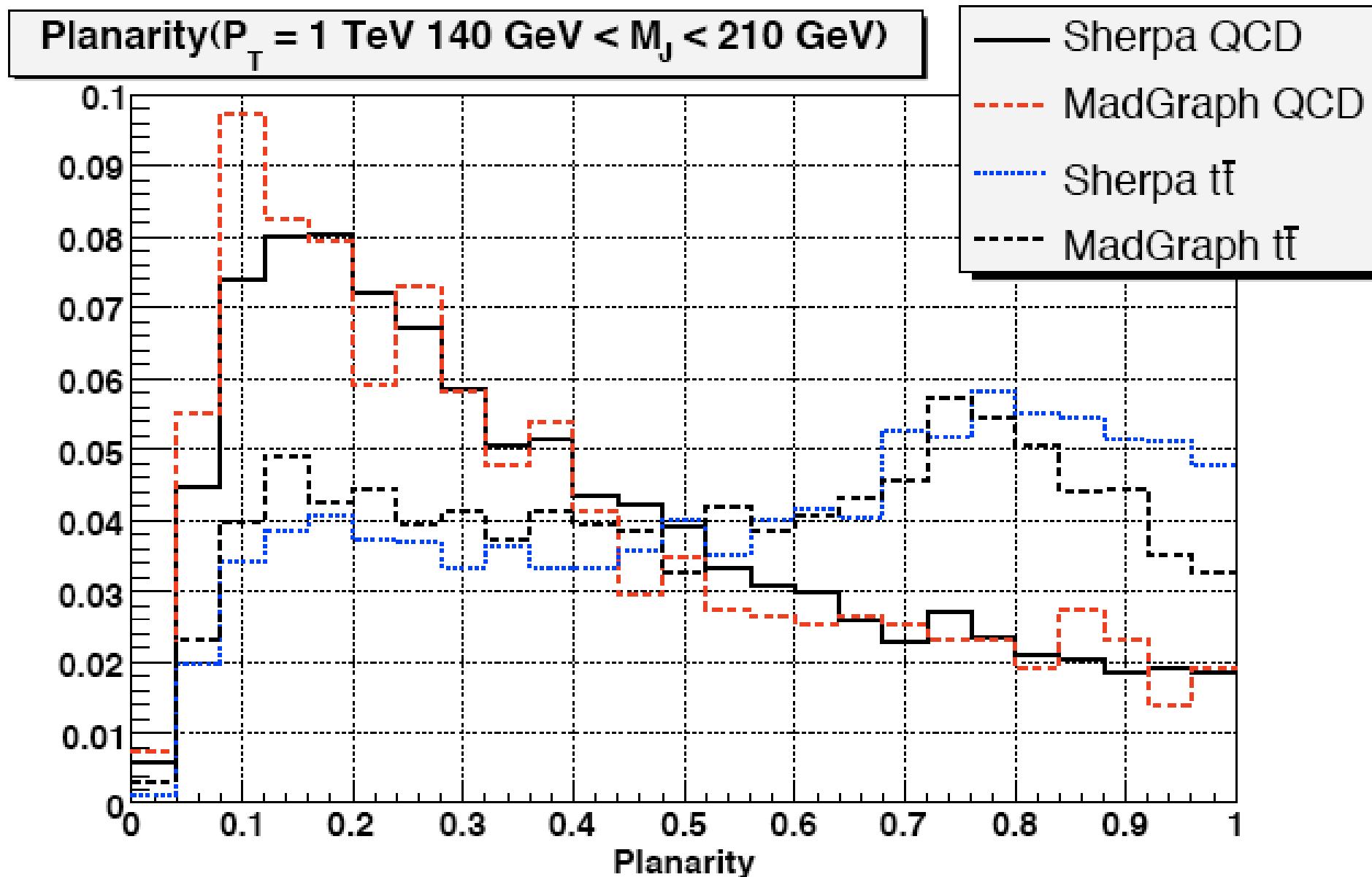


# Planar flow QCD vs top jets

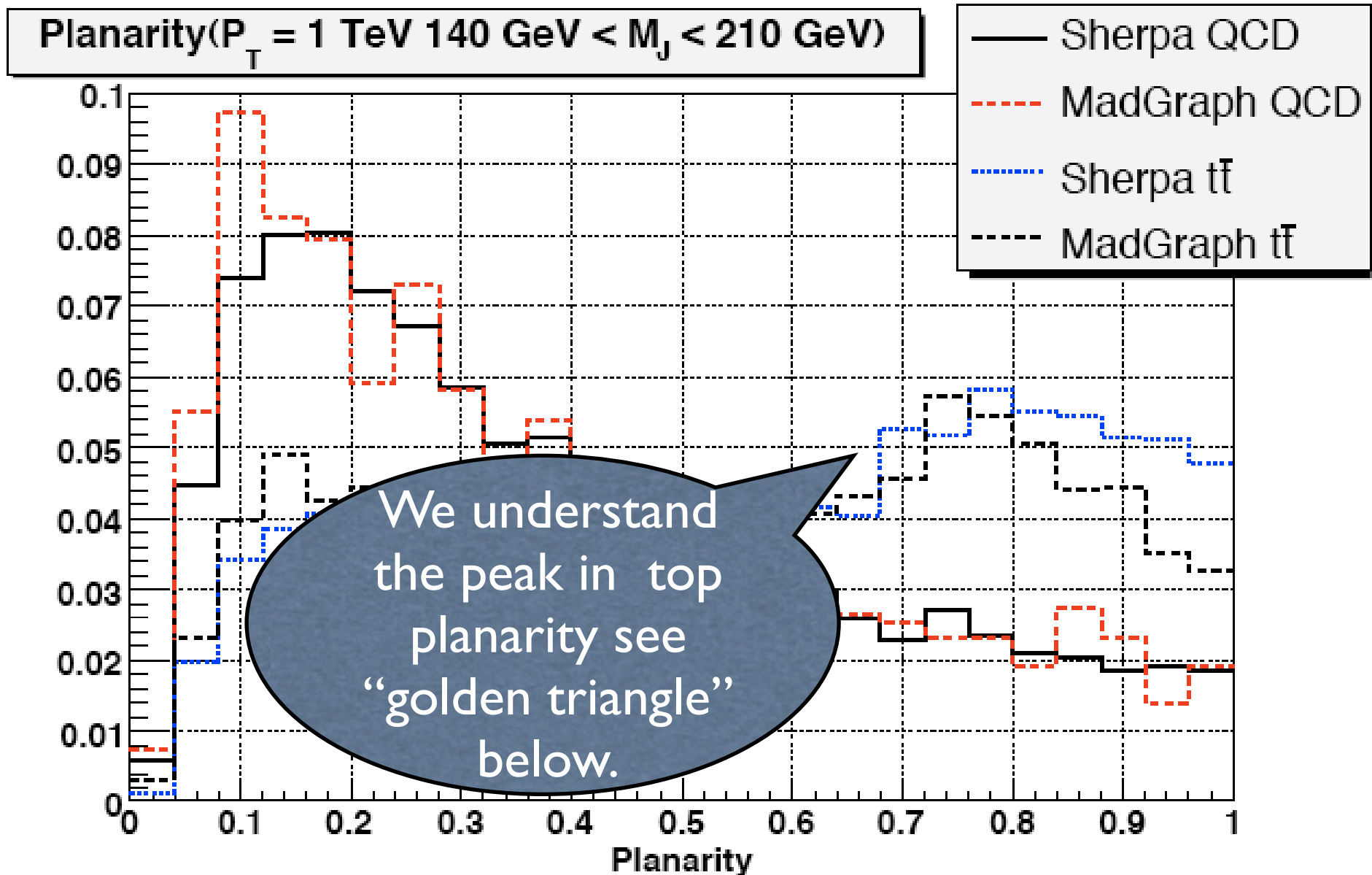
Guess: QCD planarity shows a "typical" QCD behavior, might be calculable at high planarity



# Planar flow, QCD vs top jets



# Planar flow, QCD vs top jets



# Beyond Planarity, “Probe Function”

---

- ◆ Planarity is a single variable in a 4D 3-body kinematical-variable phase-space => info' is lost.
- ◆ Can we be more systematic in our approach?  
(*Disclaimer: this part is all preliminary, under study.*)

$|t \rangle =$  top distribution

$|g \rangle =$  massless QCD distribution

We need a probe distribution,  $|f \rangle$ , such that

$$R = \left( \frac{\langle f|t \rangle}{\langle f|g \rangle} \right) \text{ is maximized.}$$

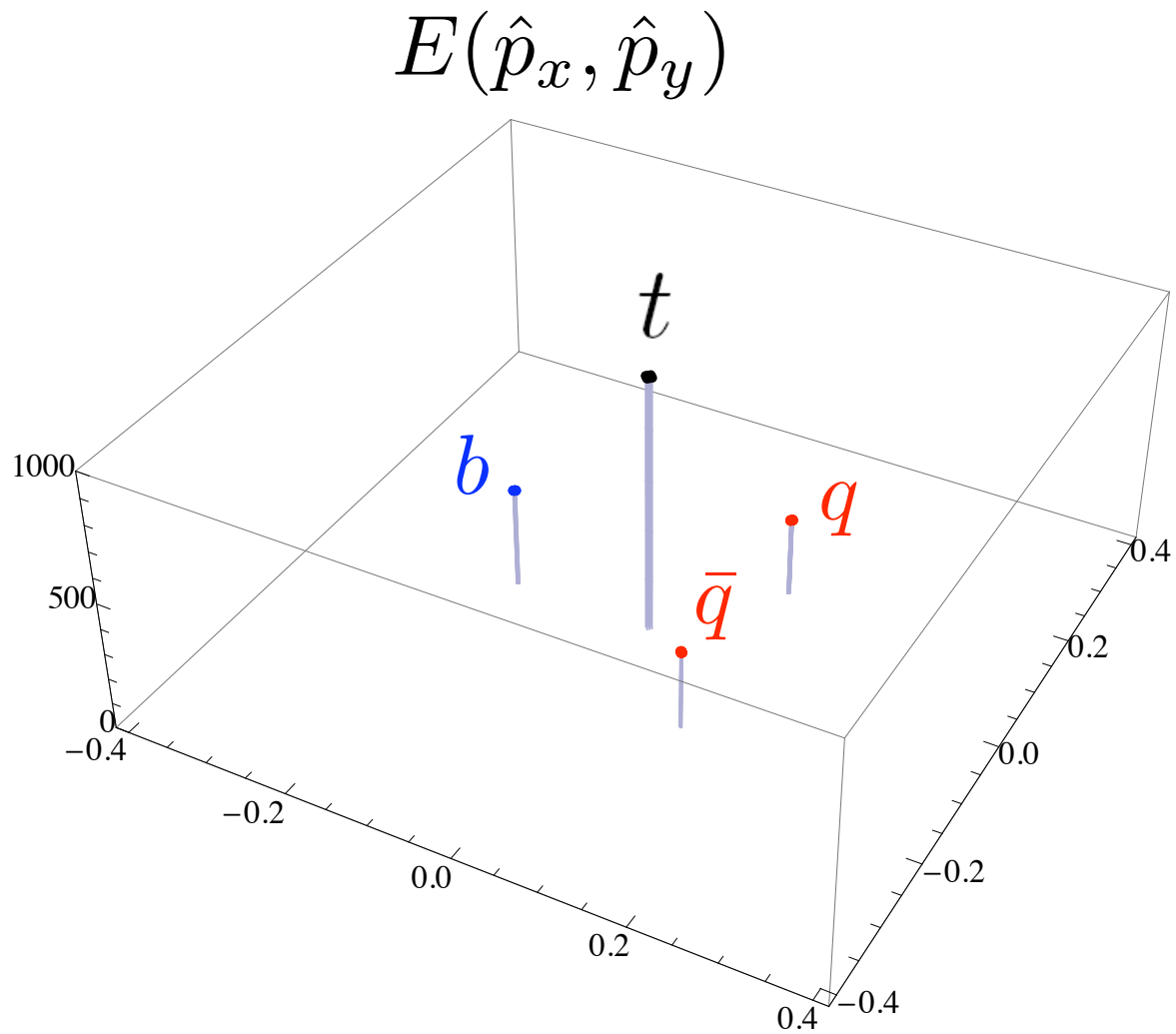
# Guess Probe Function, “Golden Triangle”

---

- ◆ Short cut, using the top dist’?
- ◆ Top dist’ is still complicated (3D), can we estimate it where it peaks,  $\theta_m^{Wb}$ ,  $\theta_m^{q\bar{q}}$  ?
- ◆ Fix one more (dummy) angle,  $\phi^{q\bar{q}}$ , to maximize planarity.
- ◆ The triangle shape is fixed up to orientation relative to the jet axis,  $\phi^{Wb}$ .

# The Golden Triangle

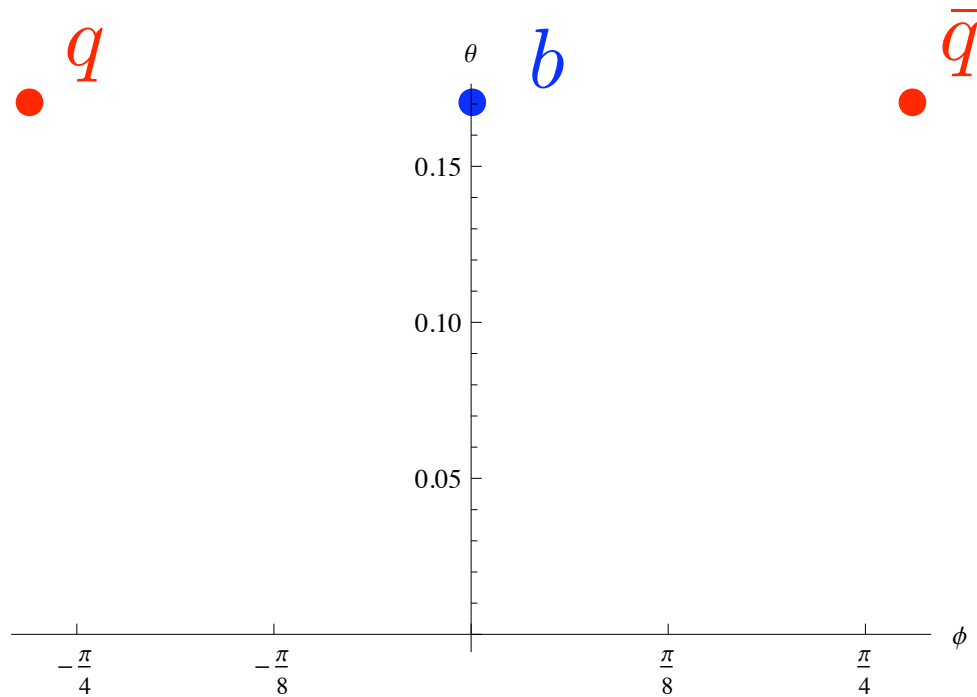
---



# The Golden Triangle

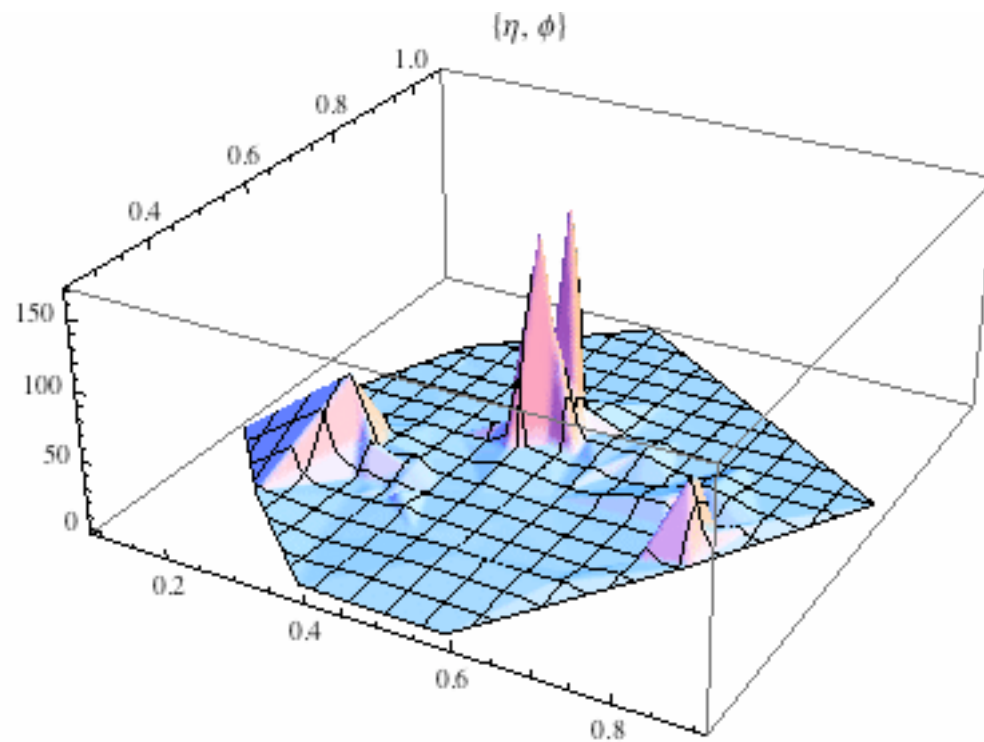
---

$\theta \sim \frac{m_t}{p_T}$  is the distance from the jet axis;  
 $\phi$  is the azimuth angle.



# The Golden Triangle & events overlap

---



# The Golden Triangle & events overlap

---

$$E_{weighted}^{b,q,\bar{q}}(\phi_b) = \int d\psi^J d\theta^J E^J(\theta^J, \psi^J) \\ \times \exp \left\{ - \left[ \frac{\theta^J(\psi^J) - \theta_{b,q,\bar{q}}}{\sqrt{2}\sigma_{\theta_{b,q,\bar{q}}}} \right]^2 \right\} \exp \left\{ - \left[ \frac{\phi_{b,q,\bar{q}}(\phi_b) - \psi^J}{\sqrt{2}\sigma_{\phi_{b,q,\bar{q}}}} \right]^2 \right\}$$

$$f = \int d\phi_b \exp \left\{ - \left[ \frac{E_{weighted}^b(\phi_b) - E_b}{\sqrt{2}\sigma_{E_b}} \right]^2 \right\} \exp \left\{ - \left[ \frac{E_{weighted}^q(\phi_b) - E_q}{\sqrt{2}\sigma_{E_q}} \right]^2 \right\} \\ \times \exp \left\{ - \left[ \frac{E_{weighted}^{\bar{q}}(\phi_b) - E_{\bar{q}}}{\sqrt{2}\sigma_{E_{\bar{q}}}} \right]^2 \right\}$$

where  $\theta_q = \theta_{\bar{q}} = \theta_b$  on the golden triangle, however  $\phi_{b,q,\bar{q}}$  are not the same since the triangle is defined once  $\phi_b$  is defined hence there is only a  $\phi_b$  integral and  $\phi_{q,\bar{q}}(\phi_b)$  are trivial functions of  $(\phi_b)$  as we have calculated these on the triangle (and of course  $\phi_b(\phi_b) = \phi_b$ ).

# Conclusions

---

- ◆ LHC => new era, precision top physics.
- ◆ Theory+technique to tag t/W/Z/h jets
- ◆ Calculation via PQCD, new insights.  
(not blindly dep' on MC).
- ◆ Remove BG better sig', increased NP sensitivity (briefly mentioned). Full det' sim'??
- ◆ Complimentary methods, algorithms to interpolate between 3-jet/2jet/t-jets

*Backups*



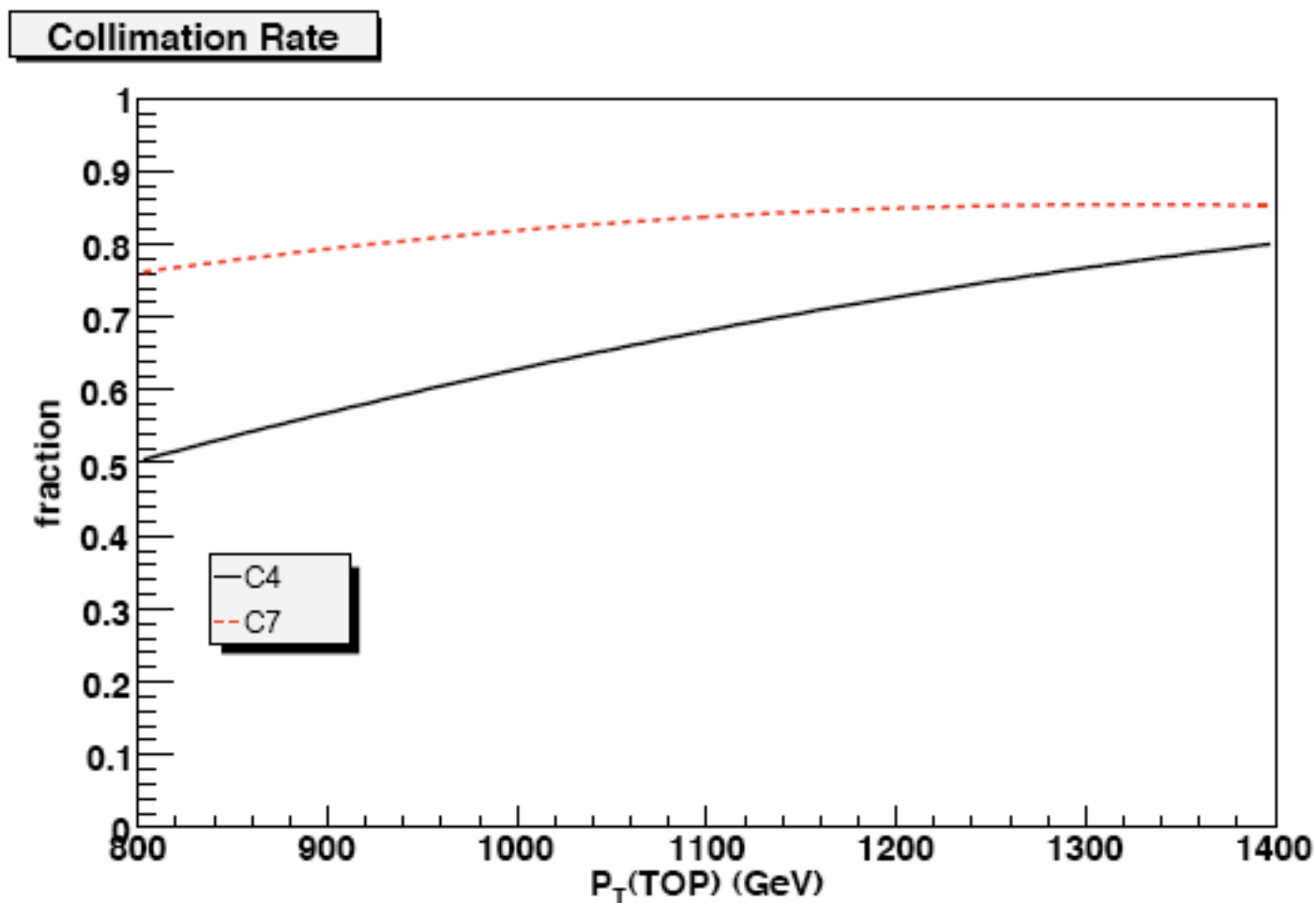
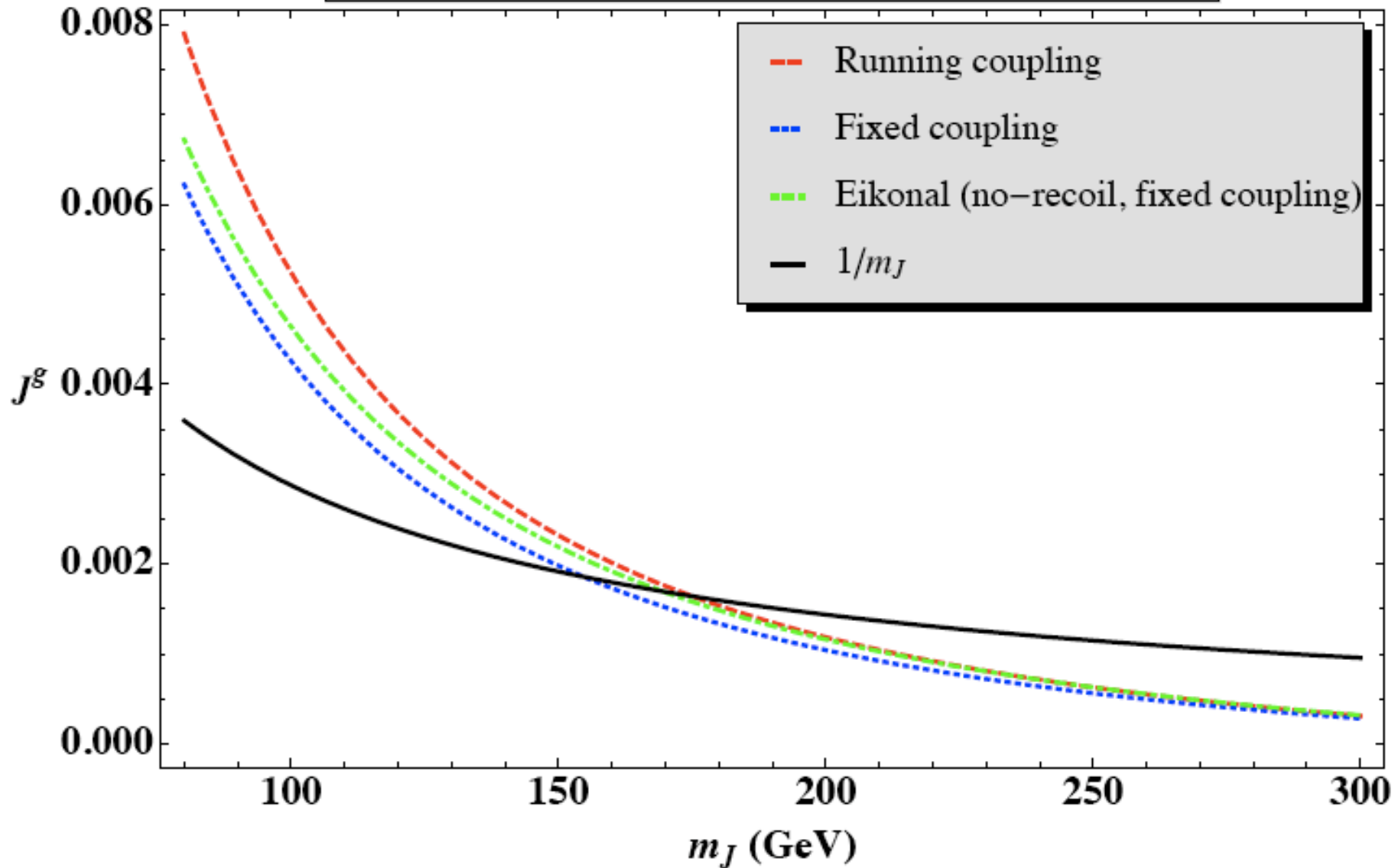


Figure 8: The collimation rate for top quarks as a function of their transverse momentum, for C4 (black solid curve) and C7 (red dashed curve) jets. Collimation rate is defined as the fraction of top quarks with  $140 \text{ GeV} \leq m_J \leq 210 \text{ GeV}$ .

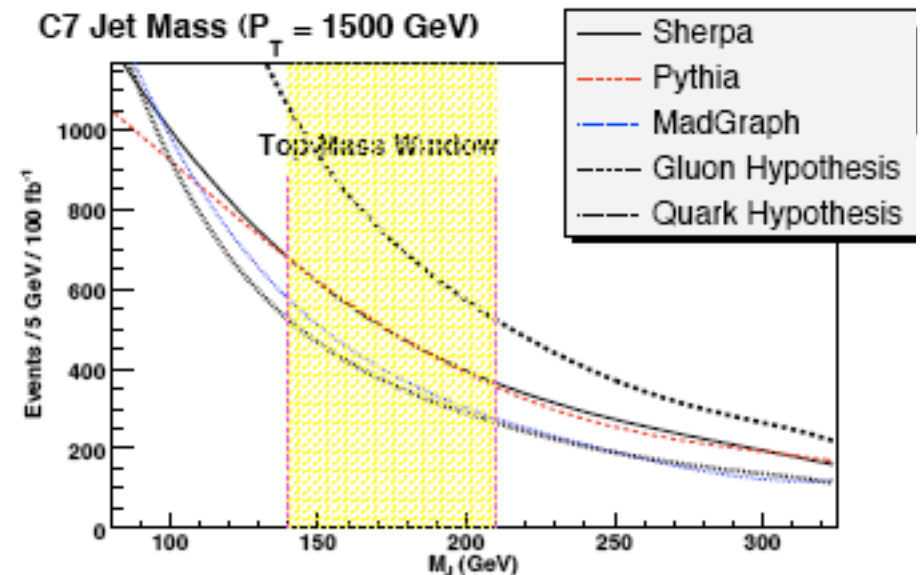
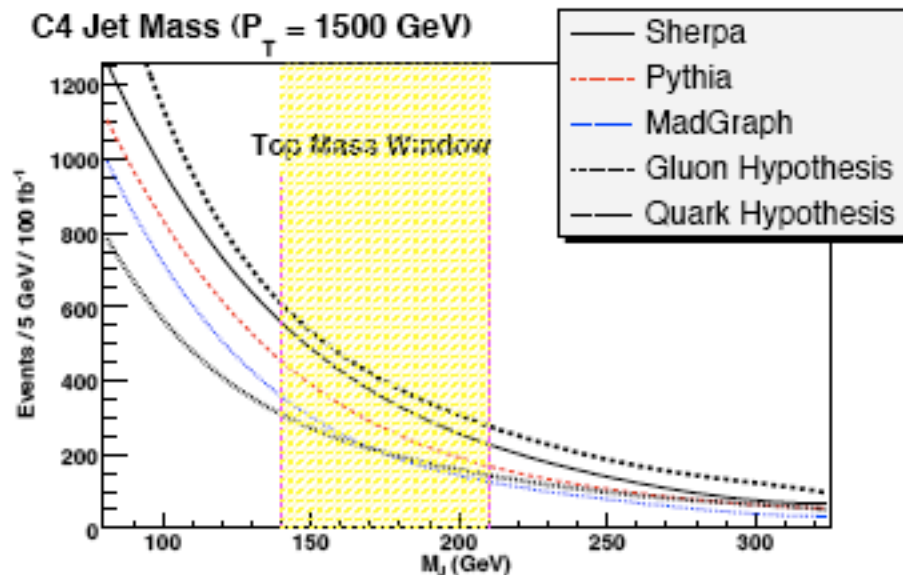
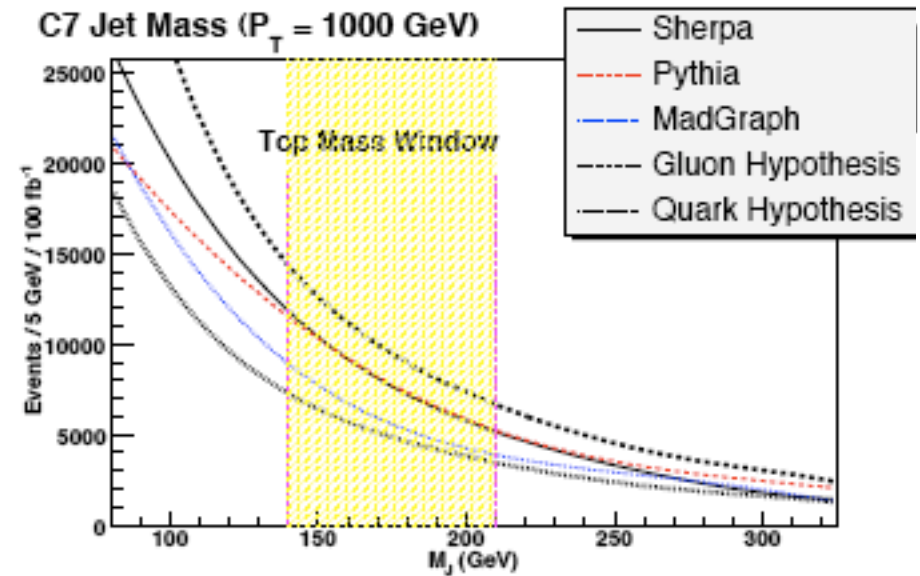
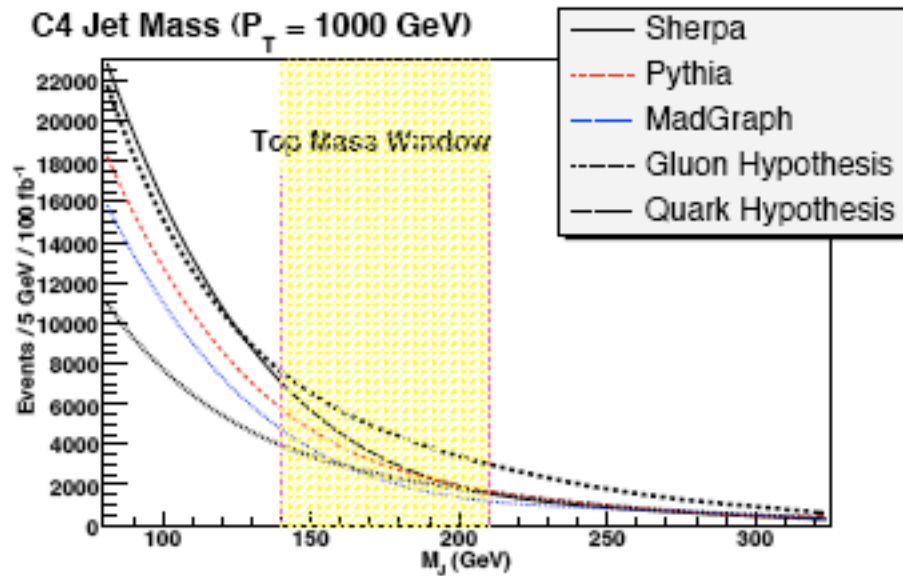
# Comparing jet function approx'

$$J^g = \frac{1}{\sigma} \frac{d\sigma}{dm_J} \quad (\text{Gluon Jet Functions, } P_T = 1 \text{ TeV, } R=0.4)$$

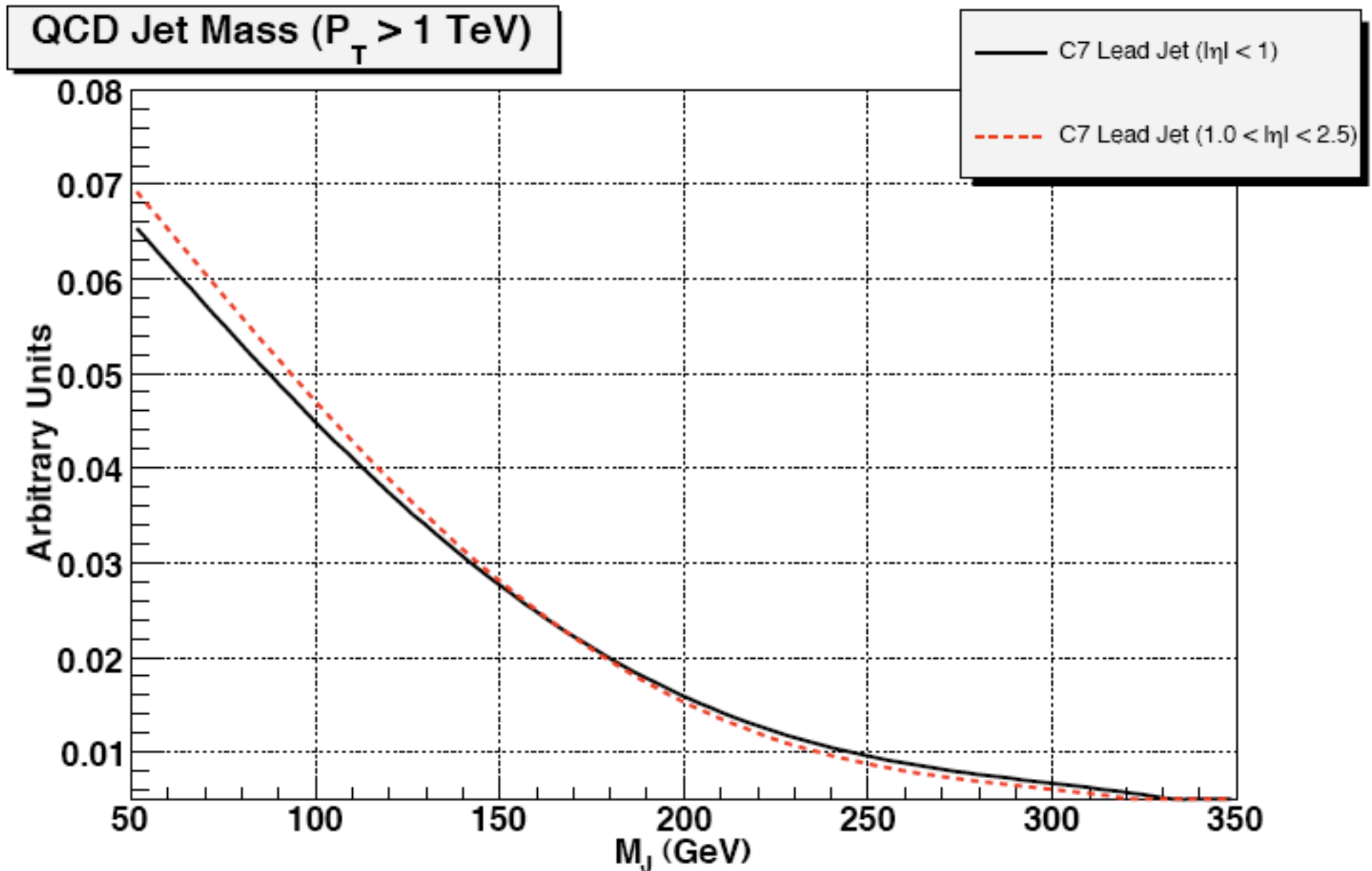


# Jet mass distribution, theory vs. MC

Various MCs, at fixed  $p_T$

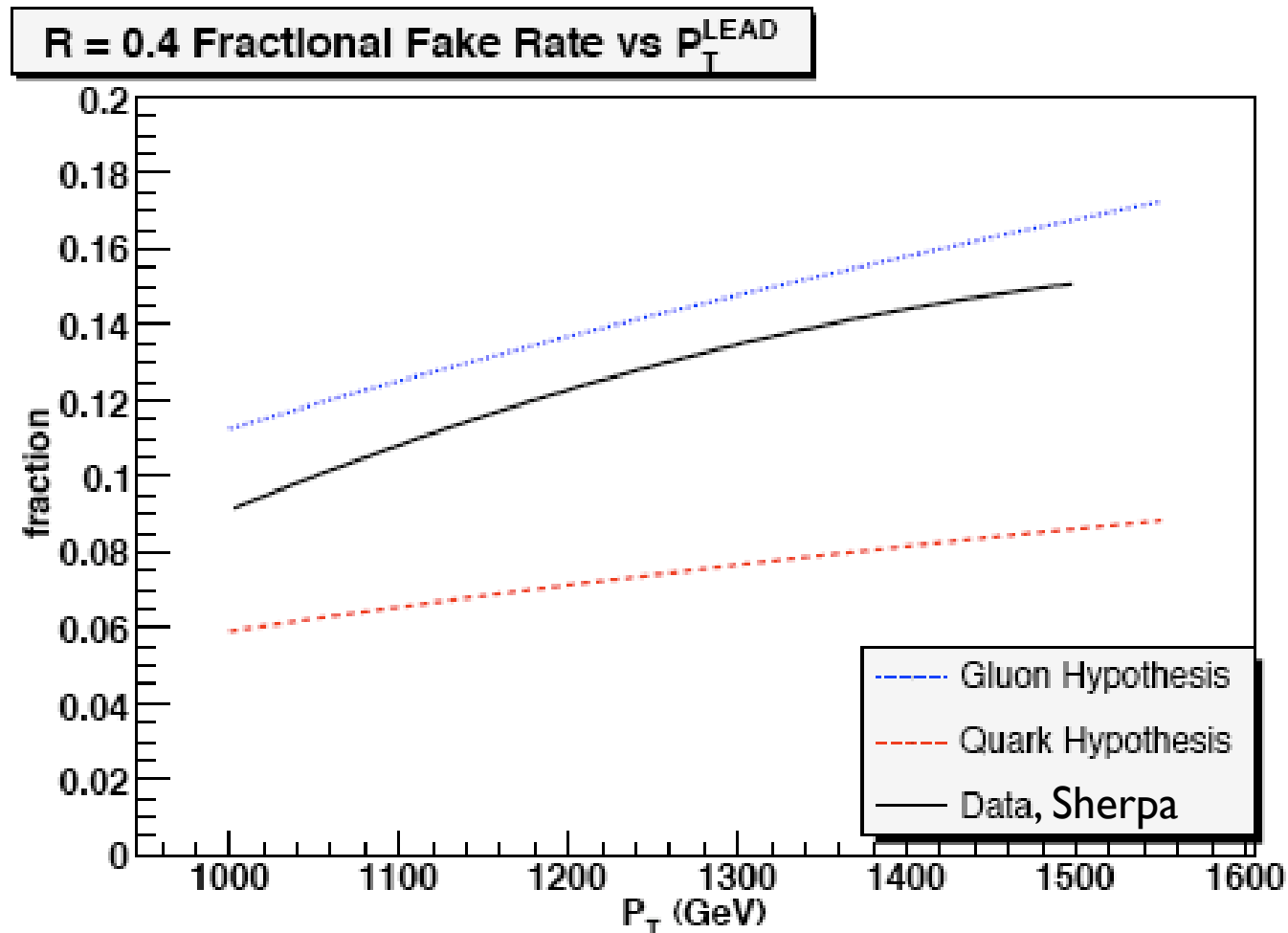


# Pseudo-rapidity independence



# Bound fake rate (# of jets in top mass window)

$$\int_{140 \text{ GeV}}^{210 \text{ GeV}} dm_J J^q(m_J, p_T, R) \leq \text{Fractional fake rate} \leq \int_{140 \text{ GeV}}^{210 \text{ GeV}} dm_J J^g(m_J, p_T, R).$$



# Naive mass tagging + detector effects

$p_T^{lead}$ cut	Cone	$S$ (0% JES)	$\Delta_0$	+5% JES	$\Delta_5$	-5% JES	$\Delta_{-5}$
1000 GeV	C4	5778	-15.8%	6562	-4.3%	4798	-30.1%
1000 GeV	C7	7367	-15.6%	8543	-2.1%	6037	-30.8%
1500 GeV	C4	741	17.6%	934	48.3%	536	-14.9%
1500 GeV	C7	789	14.5%	1119	62.4%	601	-12.8%

$p_T^{lead}$ cut	Cone	$B$ (0% JES)	$\Delta_0$	+5% JES	$\Delta_5$	-5% JES	$\Delta_{-5}$
1000 GeV	C4	107661	-5.4%	122291	7.5%	90232	-20.7%
1000 GeV	C7	192710	-2.7%	224666	13.5%	154733	-21.8%
1500 GeV	C4	13615	23.9%	18144	65.2%	10108	-8.0%
1500 GeV	C7	18712	33.7%	25361	81.2%	13407	-4.2%

$\Delta_{JES} = \frac{N_{JES} - N_{TRUTH}}{N_{TRUTH}}$ , Simple  $S/\sqrt{B}$  is not adequate.

# Naive mass tagging + detector effects

$p_T^{lead}$ cut	Cone	$S$ (0% JES)	$\Delta_0$	+5% JES	$\Delta_5$	-5% JES	$\Delta_{-5}$
1000 GeV	C4	5778	-15.8%	6562	-4.3%	4798	-30.1%
1000 GeV	C7	7367	-15.6%	8543	-2.1%	6037	-30.8%
1500 GeV	C4	741	17.6%	934	48.3%	536	-14.9%
1500 GeV	C7	789	14.5%	1119	62.4%	601	-12.8%
$p_T^{lead}$ cut	Cone	$B$ (0% JES)	$\Delta_0$	+5% JES	$\Delta_5$	-5% JES	$\Delta_{-5}$
1000 GeV	C4	107661	-5.4%	122291	7.5%	90232	-20.7%
1000 GeV	C7	192710	-2.7%	224666	13.5%	154733	-21.8%
1500 GeV	C4	13615	23.9%	18144	65.2%	10108	-8.0%
1500 GeV	C7	18712	33.7%	25361	81.2%	13407	-4.2%

$\Delta_{JES} = \frac{N_{JES} - N_{TRUTH}}{N_{TRUTH}}$ , Simple  $S/\sqrt{B}$  is not adequate.

# Results for leading jet, side band

$p_T^{\text{lead}} \geq 1000 \text{ GeV}$  Cone  $R = 0.7$   $25 \text{ fb}^{-1}$

JES	$B_{\text{FIT}}$	$S_{\text{FIT}}$	$\Delta S$	$n_\sigma$	p-value	$\chi^2/ndf$	$(S/B)_{\text{FIT}}$
0%	47277	2730	399	6.8	0.98	0.38	0.058
5%	54870	3419	424	8.1	0.87	0.60	0.062
-5%	37910	2274	354	6.4	1.00	0.21	0.060

$p_T^{\text{lead}} \geq 1500 \text{ GeV}$  Cone  $R = 0.7$   $100 \text{ fb}^{-1}$

JES	$B_{\text{FIT}}$	$S_{\text{FIT}}$	$\Delta S$	$n_\sigma$	p-value	$\chi^2/ndf$	$(S/B)_{\text{FIT}}$
0%	18456	1045	252	4.2	0.75	0.72	0.057
5%	24921	1559	284	5.4	0.96	0.45	0.063
-5%	13315	693	213	3.3	1.00	0.20	0.052

$S_{\text{FIT}}$  and  $B_{\text{FIT}}$  are the results of an extended maximum likelihood fit.  $\Delta S$  is the error on  $S_{\text{FIT}}$ .

# Results for leading jet, side band

$p_T^{\text{lead}} \geq 1000 \text{ GeV}$  Cone  $R = 0.7$   $25 \text{ fb}^{-1}$

JES	$B_{\text{FIT}}$	$S_{\text{FIT}}$	$\Delta S$	$n_\sigma$	p-value	$\chi^2/ndf$	$(S/B)_{\text{FIT}}$
0%	47277	2730	399	6.8	0.98	0.38	0.058
5%	54870	3419	424	8.1	0.87	0.60	0.062
-5%	37910	2274	354	6.4	1.00	0.21	0.060

$p_T^{\text{lead}} \geq 1500 \text{ GeV}$  Cone  $R = 0.7$   $100 \text{ fb}^{-1}$

JES	$B_{\text{FIT}}$	$S_{\text{FIT}}$	$\Delta S$	$n_\sigma$	p-value	$\chi^2/ndf$	$(S/B)_{\text{FIT}}$
0%	18456	1045	252	4.2	0.75	0.72	0.057
5%	24921	1559	284	5.4	0.96	0.45	0.063
-5%	13315	693	213	3.3	1.00	0.21	0.060

$S_{\text{FIT}}$  and  $B_{\text{FIT}}$  are the results of likelihood fit.  $\Delta S$  is the error

reasonable  
significance-  
reach

# Results for leading jet, side band

For the subleading jet we simply require mass cut (no  $p_T$  cut)

$$p_T^{\text{lead}} \geq 1500 \text{ GeV} \quad \text{Cone } R = 0.4 \quad 100 \text{ fb}^{-1}$$

JES	$B_{\text{FIT}}$	$S_{\text{FIT}}$	$\Delta S$	$n_\sigma$	p-value	$\chi^2/ndf$	$(S/B)_{\text{FIT}}$
0%	2341	430	94	4.6	0.99	0.35	0.184
5%	2968	624	110	5.7	0.96	0.45	0.210
-5%	1593	436	79	5.5	0.82	0.66	0.274

